In vivo transduction of primitive mobilized hematopoietic stem cells after intravenous injection of integrating adenovirus vectors

Richter, M. and Saydaminova, K. and Yumul, R. and Krishnan, R. and Liu, J. and Nagy, E.E. and Singh, M. and Izsvak, Z. and Cattaneo, R. and Uckert, W. and Palmer, D. and Ng, P. and Haworth, K.G. and Kiem, H.P. and Ehrhardt, A. and Papayannopoulou, T. and Lieber, A.

Blood
2016 NOV 03 ; 128(18): 2206-2217
2016 AUG 23 (first published online: accepted manuscript)
doi: 10.1182/blood-2016-04-711580

Publisher: The American Society of Hematology

GENE THERAPY

In vivo transduction of primitive mobilized hematopoietic stem cells after intravenous injection of integrating adenovirus vectors

Maximilian Richter,[1] Kamola Saydaminova,[1] Roma Yumul,[1] Rohini Krishnan,[1] Jing Liu,[2] Eniko-Eva Nagy,[3] Manvendra Singh,[3] Zsuzsanna Izsvák,[3] Roberto Cattaneo,[4] Wolfgang Uckert,[3,5] Donna Palmer,[6] Philip Ng,[6] Kevin G. Haworth,[7] Hans-Peter Kiem,[7] Anja Ehrhardt,[2] Thalia Papayannopoulou,[8] and André Lieber[1,9]

[1]Division of Medical Genetics, Department of Medicine, University of Washington, Seattle, WA; [2]Institute for Virology and Microbiology, University Witten/Herdecke, Witten, Germany; [3]Mobile DNA Group, Max-Delbrück Center for Molecular Medicine, Berlin, Germany; [4]Department of Molecular Medicine, The Mayo Clinic, Rochester, MN; [5]Molecular Cell Biology and Gene Therapy Group, Institute of Biology, Humboldt University, Berlin, Germany; [6]Department of Molecular and Human Genetics, Baylor College of Medicine, Houston, TX; [7]Clinical Research Division, Fred Hutchinson Cancer Research Center, Seattle, WA; [8]Division of Hematology, Department of Medicine, and [9]Department of Pathology, University of Washington, Seattle, WA

Key Points

- Mobilized hematopoietic stem cells transduced with IV injected HD-Ad5/35^{++} vectors home to the BM persist long term.
- Our approach allows for the stable genetic modification of primitive, long-term persisting HSPCs.

Current protocols for hematopoietic stem/progenitor cell (HSPC) gene therapy, involving the transplantation of ex vivo genetically modified HSPCs are complex and not without risk for the patient. We developed a new approach for in vivo HSPC transduction that does not require myeloablation and transplantation. It involves subcutaneous injections of granulocyte-colony-stimulating factor/AMD3100 to mobilize HSPCs from the bone marrow (BM) into the peripheral blood stream and the IV injection of an integrating, helper-dependent adenovirus (HD-Ad5/35^{++}) vector system. These vectors target CD46, a receptor that is uniformly expressed on HSPCs. We demonstrated in human CD46 transgenic mice and immunodeficient mice with engrafted human CD34^{+} cells that HSPCs transduced in the periphery home back to the BM where they stably express the transgene. In hCD46 transgenic mice, we showed that our in vivo HSPC transduction approach allows for the stable transduction of primitive HSPCs. Twenty weeks after in vivo transduction, green fluorescent protein (GFP) marking in BM HSPCs (Lin^{-}Sca1^{+}Kit^{-} cells) in most of the mice was in the range of 5% to 10%. The percentage of GFP-expressing primitive HSPCs capable of forming multilineage progenitor colonies (colony-forming units [CFUs]) increased from 4% of all CFUs at week 4 to 16% at week 12, indicating transduction and expansion of long-term surviving HSPCs. Our approach was well tolerated, did not result in significant transduction of nonhematopoietic tissues, and was not associated with genotoxicty. The ability to stably genetically modify HSPCs without the need of myeloablative conditioning is relevant for a broader clinical application of gene therapy. (*Blood*. 2016;128(18):2206-2217)

Introduction

Hematopoietic stem/progenitor cells (HSPCs) are an important gene therapy target, as recent clinical trials have shown clear therapeutic benefits for otherwise incurable blood diseases.[1] Current HSPC gene therapy protocols involve the transplantation of ex vivo lentivirus vector transduced HSPCs and are associated with a number of drawbacks. Ex vivo culturing of HSPCs in the presence of multiple cytokines can affect their multipotency and engraftment potential. Furthermore, most protocols involve myeloablation resulting in blood-cell depletion and susceptibility to infections and mucosal damage. Thus, the development of an in vivo HSPC transduction approach, circumventing conditioning and transplantation would be highly desirable.

Direct transduction of HSPCs localized in the bone marrow (BM) is inefficient because of physical barriers formed by the BM stroma. Mobilization, an enforced egress of HSPCs from the BM, can be achieved by a variety of approaches.[2] A combination of granulocyte colony-stimulating factor (G-CSF) and the CXCR4 antagonists AMD3100 (Mozobil, Plerixa) has been shown to efficiently mobilize primitive progenitor cells in animal models and in humans.[3] A problem for in vivo HSPC transduction is the low number of HSPCs in the BM. Only about 1 in 10^{8} nucleated marrow cells are HSPCs[4]; the vast majority of cells in the BM are blood cell progenitor cells with different levels of lineage commitment. A long-term therapeutic effect of gene therapy requires that gene transfer vectors target these rare HSPCs.

CD46 complement regulatory protein is expressed on all human HSPCs.[5] We identified CD46 as the high-affinity receptor for a number of adenoviruses (Ads), including serotype 11, 16, 21, 35, and 50.[6] The receptor interacting moiety in the capsid of Ads is the C-terminal globular trimeric fiber domain, called the fiber knob. Both others and we have shown that Ad vectors containing the Ad35 fiber or fiber knob (Ad5/35) efficiently transduce human and non-human primate HSPCs in vitro.[7-10]

Submitted 18 April 2016; accepted 10 August 2016. Prepublished online as *Blood* First Edition paper, 23 August 2016; DOI 10.1182/blood-2016-04-711580.

The online version of this article contains a data supplement.

There is an Inside *Blood* Commentary on this article in this issue.

The publication costs of this article were defrayed in part by page charge payment. Therefore, and solely to indicate this fact, this article is hereby marked "advertisement" in accordance with 18 USC section 1734.

Materials and methods

Reagents

G-CSF/Filgrastim was from Amgen (Thousand Oaks, CA). AMD3100 was from Sigma (St. Louis, MO).

Ad vectors

The first-generation Ad5/35^{++}-green fluorescent protein (GFP) vector,[11] Ad5-GFP vector,[8] and the Sleeping Beauty (SB) 100× transposase encoding helper-dependent adenovirus (HD-Ad)-SB vectors[12] are described elsewhere. Generation of the transposon vector HD-Ad–GFP genome using a recombineering strategy[13] is described in detail in the supplemental Methods (see "Adenovirus vectors"), available on the *Blood* Web site.

Cells

Human CD34^{+}-enriched cells from G-CSF mobilized normal donors were obtained from the Fred Hutchinson Cancer Research Center Cell Processing Core Facility and cultured as described previously.[8] Colony-forming unit (CFU) assays were performed using ColonyGEL (ReachBio, Seattle, WA) human or mouse complete medium according to the manufacturer's specifications.

Tissue immunofluorescence analysis

Before tissue harvest, blood was flushed from the circulation with phosphate buffered saline using the heart as a pump. Tissues were frozen in optimal cutting temperature compound. Sections (6 μm) were fixed in 4% paraformaldehyde and either remained unstained or was stained with rat anti-mouse CD45 primary antibody (Ab) (BD Biosciences, Franklin Lakes, NJ). Specific binding of primary Abs was visualized with secondary anti-rat Alexa Fluor 488 Ab. After washing, the slides were mounted with Vectashield containing 4′,6-diamidino-2-phenylindole (DAPI) (Vector Laboratories, Inc., Burlingame, CA). Immunofluorescence microphotographs were taken at room temperature on a Leica DMLB microscope (40× oil lens) (Leica, Wetzlar, Germany) with a Leica DFC300FX digital camera and Leica Application Suite version 2.4.1 R1 (Leica Microsystems, Heerbrugg, Switzerland).

Integration site analysis

Genomic DNA was isolated from GFP^{+} hCD46tg colonies using the DNeasy Blood and Tissue Kit (Qiagen, Valencia, CA). These CFU colonies were obtained from Lin^{-}/GFP^{+} BM cells of in vivo transduced hCD46tg animals. Amplification of SB genomic DNA junctions was performed by linear amplification-mediated polymerase chain reaction (PCR) as described previously[14] and in detail in the supplemental Methods (see "Construction of integration site libraries").

Mouse studies

hCD46-transgenic mice

C57Bl/6 based transgenic mice that contained the human CD46 genomic locus and provide CD46 expression at a level and in a pattern similar to humans were described earlier.[15]

Mobilization and in vivo transduction. HSPCs were mobilized in mice by subcutaneous (SC) injections of human recombinant G-CSF (5 mg/d per mouse, 4 days), followed by an SC injection of AMD3100 (5 mg/kg) on day 5. In addition, animals received dexamethasone (10 mg/kg) intraperitoneally (IP) 16 hours and 2 hours before virus injection. Forty minutes after AMD3100, animals were IV injected with Ad vectors through the retro-orbital plexus with a total dose of 4×10^{10} viral particles (vp). In double injection settings, animals received up to 4×10^{10} vp twice at 30 minutes and 60 minutes after AMD3100 injection.

Secondary BM transplantation. Recipients were female C57BL/6 mice, 6 to 8 weeks old. On the day of transplantation, recipient mice were irradiated with 1000 Rad. BM cells from in vivo transduced hCD46tg mice were isolated aseptically and GFP^{+} cells were isolated using fluorescence-activated cell sorting. Four hours after irradiation, GFP^{+} cells were IV injected through the tail vein at 1×10^{6} cells per mouse.

Generation of humanized non-obese diabetic/severe combined immunodeficiency/interleukin (IL)-2Rγnull (NOG) mice. The immunodeficient NOG mice were obtained from The Jackson Laboratory (Bar Harbor, ME). NOG recipient mice received 300 Rad whole body irradiation; 2.5×10^{5} whole BM cells of non-irradiated NOG mice were mixed with 3×10^{5} human CD34^{+} cells and IV injected into recipient mice at 4 hours post-irradiation.

Results

Transient in vivo transduction of mobilized BM cells with a first-generation Ad5/35^{++} vector

Although CD46 is expressed on all nucleated cells in humans, the corresponding mouse ortholog is only expressed in the testes. For in vivo HSPC transduction studies, a transgenic mouse model (hCD46tg) expressing hCD46 in a pattern and at a level similar to humans was used.[15] In hCD46tg mice, hCD46 is expressed at high levels in BM HSPCs (Figure 1A). This fraction is depleted for blood lineage cells (Lin^{-}) and positive for c-Kit and Sca-1 (so called Lin^{-}Sca1^{+}Kit^{+} [LSK] cells).[16] hCD46 expression was higher on LSK than on more differentiated Lin^{-} and total mononuclear cells (MNCs). We employed G-CSF/AMD3100 to mobilize HSPCs from the BM of hCD46tg mice. Mobilization resulted in a ~100-fold increase of LSK cells in peripheral blood at 40 minutes after AMD3100 injection as shown by flow cytometry (Figure 1B) and CFU progenitor assays (Figure 1C).

Initial transduction studies employed an affinity-enhanced first-generation Ad5/35 vector expressing GFP and carrying a modified Ad35 fiber knob with a 25-fold increased affinity to hCD46 (Ad5/35^{++}-GFP).[11] hCD46-tg mice were mobilized with G-CSF and AMD3100, and 40 minutes after AMD3100, Ad5/35^{++}-GFP was IV injected. At 2 hours after transduction, 24% of peripheral blood LSK cells were GFP^{+}, indicating efficient transduction of circulating mobilized HSPCs (Figure 1D). Direct transduction of BM and splenic LSK cells was inefficient with 0.7% and 2.7% GFP^{+} cells, respectively. Mobilized, transduced LSK cells left the periphery by day 3 after transduction (Figure 1E). At the same time, GFP^{+} LSK cells could be detected in the BM and spleen (Figure 1F). In the BM, 7.6% of LSK cells had been transduced, whereas only 0.3% of total MNCs were GFP^{+}, showing preferential transduction of HSPCs. In the spleen, 13% of LSK cells and 1.2% of total MNCs expressed GFP, respectively. Without mobilization, 0.3% and 3.5% of LSK cells in the BM and spleen, respectively, were GFP^{+} at day 3. The percentage of GFP^{+} LSK cells in the BM decreased over time with 3.4% and 2.1% positive cells at days 7 and 14, respectively. A faster decline was observed in transduced splenic LSK cells. The loss of GFP^{+} cells over time could be due to: (1) differentiation of LSK cells; (2) vector cytotoxicity associated with leaky expression of viral genes from the first-generation Ad5/35^{++}-GFP genomes[17]; (3) loss of episomal, non-integrated Ad vector genomes during cell division; and/or (4) competition by nontransduced HSPCs.

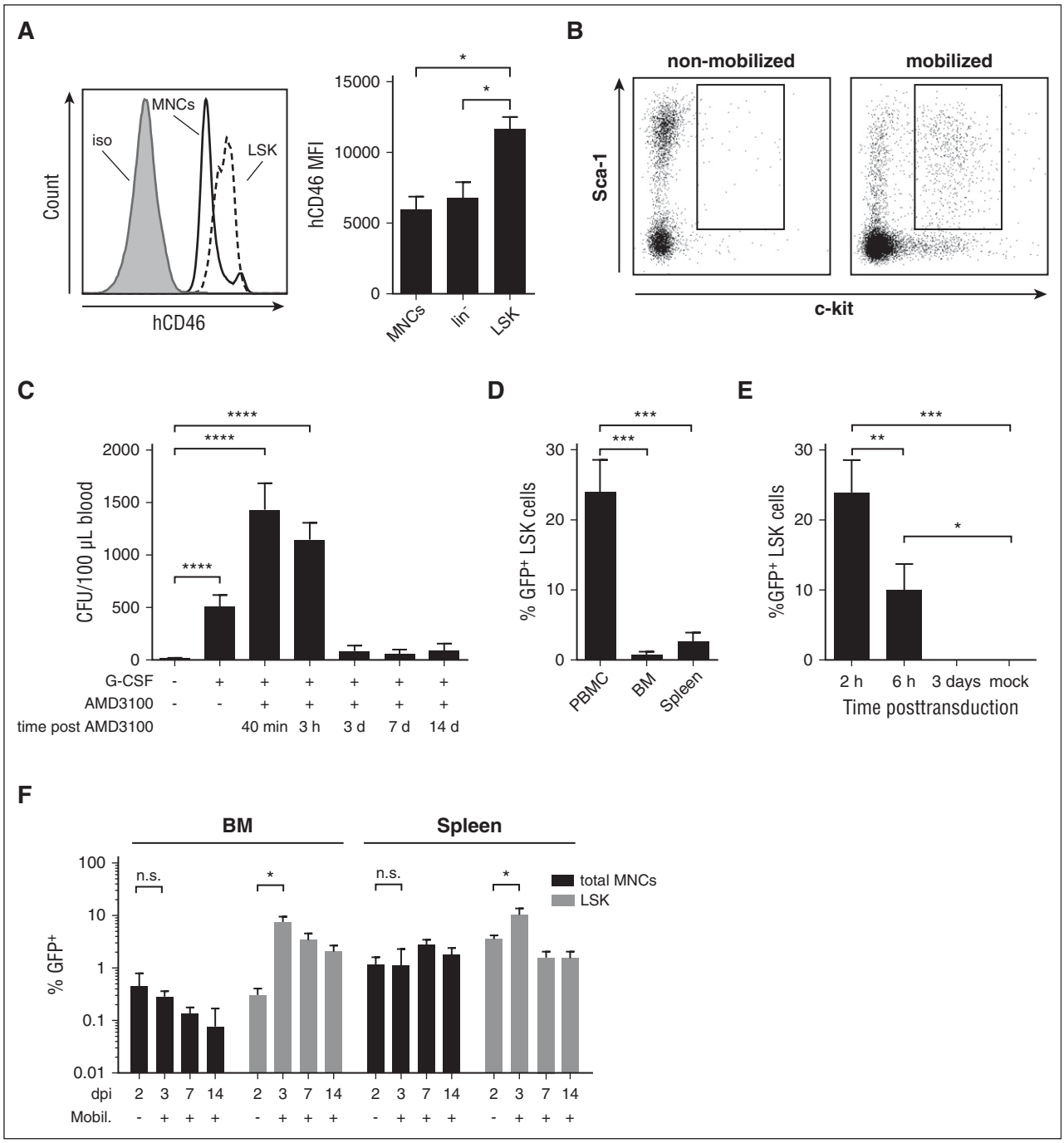

Figure 1. In vivo transduction of mobilized HSPCs with a first-generation Ad5/35^{++} vector after mobilization. (A) hCD46 expression on BM total MNCs, lineage-depleted BM cells (Lin$^-$), and LSK cells from hCD46tg mice. Representative hCD46 flow cytometry analysis with MNC (solid black) and LSK cells (dashed black) (left). The gray curve represents MNCs stained with an isotype-matched control. hCD46 MFI on MNCs, Lin$^-$, and LSK cells (right). N = 3. *$P < .05$, after one-way analysis of variance (ANOVA) with Tukey's multiple comparison test. (B) Mobilization of LSK cells in hCD46tg mice by SC G-CSF injection for 4 days, followed by a single SC injection of AMD3100 on day 5. Forty minutes after the AMD3100 injection, PBMCs were harvested and analyzed by flow cytometry for LSK cells. Representative plots of nonmobilized and mobilized mice are shown. (C) Analysis of HSPC mobilization based on CFU formation. PBMCs were collected before onset of mobilization treatment, before injection of AMD3100, 40 minutes and 3 hours after the AMD3100 injection, as well as on days 3, 7, and 14 after mobilization. The collected cells were subjected to CFU assays and colonies were enumerated 12 days after plating. Shown are mean ± standard deviation (SD), colonies normalized to a blood volume of 100 µL. N = 3. (D) A total of 4×10^{10} vp of the first-generation Ad5/35^{++}-GFP vector was IV injected 40 minutes after AMD3100. To alleviate release of pro-inflammatory cytokines associated with IV Ad vector injection, animals received dexamethasone (10 mg/kg) IP 16 hours and 2 hours before virus injection. Early transduction was analyzed by harvesting PBMCs, BM, and spleen cells at 2 hours after virus injection, and culturing them for 48 hours to allow for GFP expression. Shown is the percentage of GFP$^+$ cells in the LSK cell fractions (analyzed by flow cytometry). N = 3. (E) Animals were mobilized and injected with Ad5/35^{++}-GFP as before. Animals were euthanized and PBMCs collected at 2 hours and 6 hours after transduction. The cells were cultured for 48 hours to allow for GFP expression. Shown is the percentage of GFP$^+$ LSK cells. In addition, GFP expression in peripheral blood LSK cells was analyzed at 3 days after transduction, without culturing of the cells. Unmobilized, untransduced animals were used as controls (mock). N = 3. (F) Animals were mobilized and injected with Ad5/35^{++}-GFP as before. Transduction was analyzed by harvesting BM and splenic cells at day 3, 7, and 14 after Ad5/35^{++}-GFP injection. Nonmobilized control animals were euthanized 2 days after infection. Shown is the percentage of GFP$^+$ cells within total MNCs, and LSK cells in the BM and spleen. N = 3. Values represent means ± SD. *$P < .05$; **$P < .01$; ***$P < .001$; ****$P < .0001$, after unpaired Student *t* test comparing nonmobilized controls with animals euthanized 3 days after transduction. dpi, days postinfusion; Iso, isolated; MFI, mean fluorescence intensity; Mobil, mobilized; n.s., not significant.

Stable in vivo transduction of HSPCs with integrating HD-Ad5/35^{++} vectors

To address the problem of first-generation vector-related cytotoxicity and to allow for chromosomal integration of the transgene, we used a hyperactive SB transposase (SB100×) system in the context of HD-Ad5/35^{++} vectors that lack all viral genes. The system consists of 2 vectors (Figure 2A). The transposon vector HD-Ad–GFP contains a *GFP* gene under the control of the EF1α promoter, a promoter that is active in HSPCs. The transgene cassette is flanked by inverted repeats, which are recognized by SB100× and frt sites for circularization of the transgene cassette through Flpe recombinase. The second vector, HD-Ad–SB, supplies Flpe and SB100× in trans to mediate integration of the *GFP* cassette into a thymine-adenine dinucleotide of the genomic DNA.[18] Both vectors contain the affinity-enhanced Ad35^{++} fiber knob. In vitro studies with hCD46tg Lin$^-$ cells (supplemental Figure 1) and MO7e cells, a model cell line for human HSPCs (supplemental Figure 2), demonstrated efficient transgene integration through the SB100× vector system.

The two-vector system was then used for in vivo HSPC transduction in hCD46tg mice. First, we determined that doubling the vector dose (2 injections of each 4 × 10^{10} vp given 30 and 60 minutes after AMD3100) significantly increased the percentage of transduced LSK cells in peripheral blood ($P < .05$; supplemental Figure 3). This treatment regimen was used for all subsequent studies. For in vivo studies, mobilized animals received a combination of HD-Ad–SB and HD-Ad–GFP (Figure 2B). At 3 days after in vivo transduction, GFP expression in CD3$^+$, CD19$^+$, and Gr-1$^+$ hematopoietic lineages and HSPCs was analyzed in the BM, spleen, and peripheral blood mononuclear cells (PBMCs) (Figure 2C). This analysis showed that: (1) our vectors not only transduce mobilized LSK cells but also differentiated cells; (2) mobilization significantly increased GFP marking of LSK cells in the BM and spleen; and (3) not only transduced mobilized LSK cells but also CD19$^+$ cells appeared to return back to the BM after transduction in the periphery.

To evaluate stable long-term transgene expression after HSPC transduction, groups of mice were injected with both vectors, or HD-Ad–GFP alone and euthanized 4, 8, 12, and 20 weeks after transduction (Figure 2D). Total BM MNCs of animals injected with both vectors showed GFP in 2.5%, 1.1%, 0.4%, and 0.9% of cells at 4, 8, 12, and 20 weeks after transduction. The loss of transduced cells over time was most likely due to exit or turnover of short-term reconstituting HSPCs and differentiated cells.[19] Animals that received HD-Ad–GFP alone showed a significantly lower transduction with 0.4% at 4 weeks after transduction ($P < .001$) and transduction levels remained low at later time points. Overall, higher transduction rates were observed for BM LSK cells, again suggesting preferential transduction of more primitive cells. Up to 7.7% (average = 2.45%) of all BM cells were GFP$^+$ at week 4 after injection. The percentage of GFP$^+$ cells declined over time during week 8 and 12, and increased again at week 20 to 5% to 10% of GFP$^+$ LSK cells in most animals.

In the spleen of animals injected with both vectors, GFP was expressed in 11.8%, 17.6%, 5.7%, and 16.1% of cells at 4, 8, 12, and 20 weeks posttransduction, suggesting transient expansion of transduced cells or influx of modified, BM-derived cells.

In the blood, rapid loss of transgene expression could be observed in most animals, most likely due to anti-GFP immune responses, eliminating GFP-marked PBMCs, as supported by the occurrence of high serum titers of anti-GFP Abs and GFP-specific CD8 T cells in the spleen of mice that were euthanized at week 20 after in vivo transduction (supplemental Figure 4). Notably, stable transduction of splenocytes with the HD-Ad–GFP vector alone was also observed in some animals. Although this observation is consistent with a low frequency of integration of HD-Ad vectors through their inverted terminal repeats reported earlier,[20] it requires further investigation.

Differentiation of transduced HSPCs into lineage-positive cells is supported by the analysis of GFP expression in CD3, CD19, and Gr-1$^+$ cells present in the BM and spleen at day 3, week 8, and week 20 after transduction (Figure 2E). GFP marking of CD3 and CD19 cells in the BM was higher at week 8 than at day 3. In the spleen, increases in GFP marking over time were seen for CD19$^+$ and Gr-1$^+$ cells, suggesting an influx of modified cells derived from HSPCs in the BM, rather than initial transduction or expansion of the cells in the spleen. The fact that the CD19$^+$ cells turnover is less than 4 weeks[21,22] and that modified cells are detected at much later time points, support this hypothesis. Notably, changes in the levels of BM CD19$^+$ and Gr-1$^+$ cells were observed after in vivo transduction, independent of animals' mobilization status. In the spleen and blood however, a clear influence of the mobilization on the lineage composition was observed (supplemental Figure 5).

To support these flow cytometric analyses, a functional HSPC assay were performed. First, the ability of GFP$^+$ lineage-depleted BM cells harvested at week 4, 8, 12, and 20 after HD-Ad injection to form multilineage progenitor colonies (or CFUs) was analyzed (Figure 3A). The percentage of GFP$^+$ CFUs increased during the first 12 weeks in treated animals, suggesting enrichment of transduced colony-forming cells and the loss of transduced less primitive cells (Figure 3B). At 12 weeks after transduction, 16.5% of colony-forming cells were stably modified. At week 20, markedly fewer colonies were formed with lower rates of gene modification, most likely due to the animals' old age (~8 months), which is associated with HSPC deterioration.[23] Of 80 GFP-positive colonies screened, 30.9% were granulocyte, erythrocyte, monocyte, megakaryocyte CFU, 29.4% were granulocyte/macrophage progenitors CFU, 14.7% were granulocyte CFU, 13.2% were erythroid burst-forming unit, and 11.7% were erythroid CFU, suggesting that multipotent progenitors were efficiently transduced (Figure 3C and data not shown).

Additionally, BM of in vivo transduced hCD46tg animals was used to rescue lethally irradiated C57BL/6 recipients to assess the multilineage, long-term reconstitution potential of gene-modified HSPCs (Figure 4A). Successful engraftment, based on hCD46 expression in PBMCs, was achieved in 6 out of 7 animals (Figure 4B). GFP marking rates in PBMCs were on average 9% and remained stable (Figure 4C). At week 16, animals were euthanized and GFP marking was assessed in cells of the BM, spleen, lungs, and thymus, as well as in PBMCs. Analysis of BM showed GFP$^+$ HSPCs (Lin$^-$, LSK, and LSK SLAM) (Figure 4D). In the BM, GFP marking was seen in 5.9% of Lin$^-$ cells, in 8.6% of LSK cells, and in 4.6% of primitive LSK SLAM (LSK, CD150$^+$, CD48$^-$) cells. GFP marking was also detected in CD3, CD19, CD11b, and Gr-1$^+$ cells of the BM, spleen, and blood (Figure 4E), as well as in leukocytes in the lung and thymus (Figure 4F). Furthermore, GFP marking was detected in microglia in the brain as well as in leukocytes found in the lumen of intestinal villi of the small intestine, both most likely derived from transduced HSPCs (supplemental Figure 6). We cannot explain why after transplantation of GFP-positive HSPCs, engraftment rates were over 90%, but GFP-positive cells were only about 9%. We hypothesize that this is due to either the presence of GFP$^+$ cells without stable vector integration in the transplant or the development of anti-GFP immune responses in transplant recipients, leading to the killing of GFP-expressing PBMCs.

Taken together, the CFU and in vivo repopulation data suggest that our HD-Ad–SB + HD-Ad–GFP vector system can transduce and stably modify long-term reconstituting hematopoietic stem cells

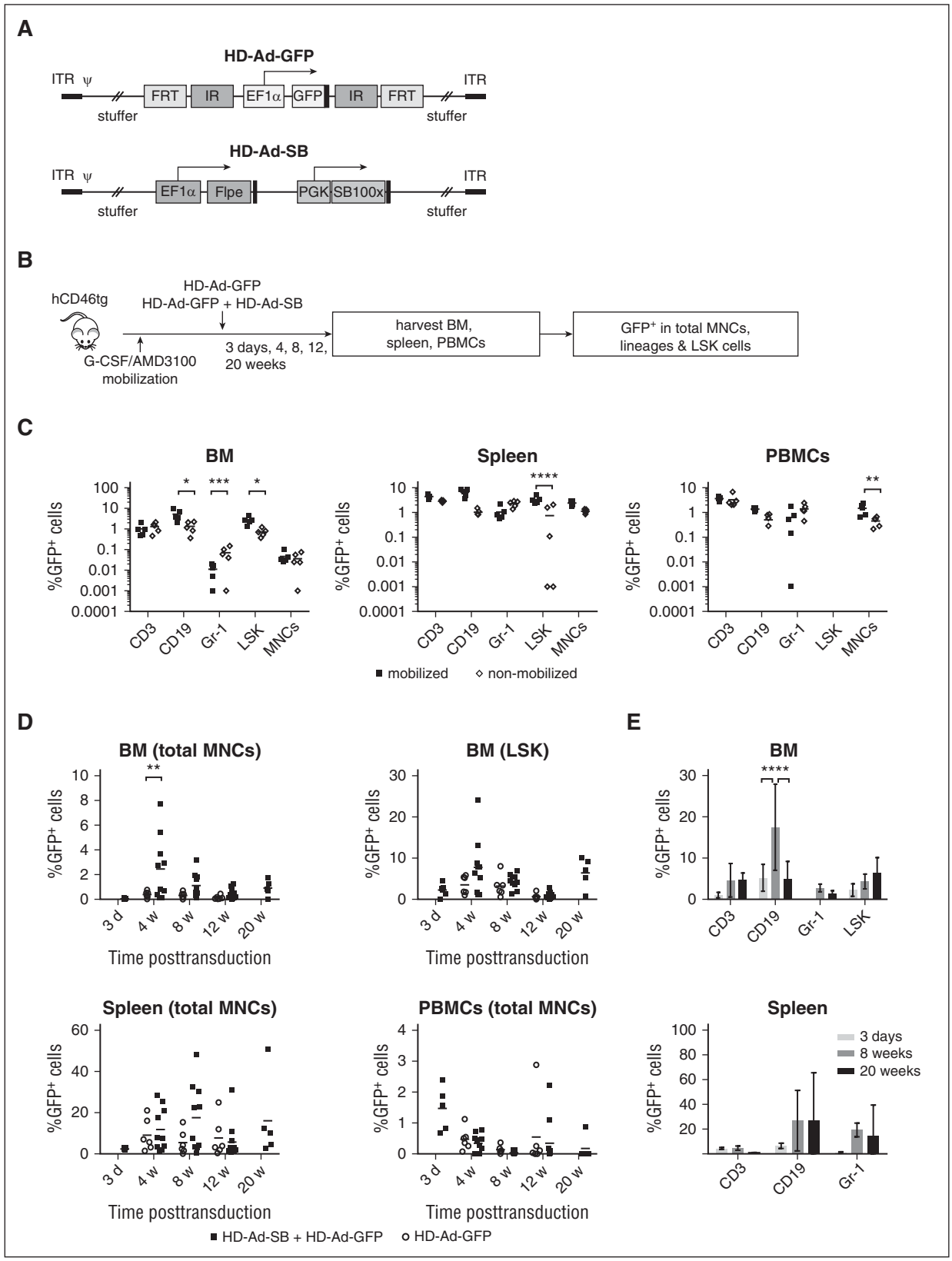

Figure 2. Stable in vivo HSPC transduction with integrating HD-Ad5/35^{++} vectors. (A) Vector genome structure. The transposon vector (HD-Ad–GFP (left) carries an Ef1α-driven GFP expression cassette that is flanked by inverted transposon repeats and *frt* sites. The second vector (HD-Ad–SB) (right) provides both Flpe recombinase and SB100× transposase in trans. Both are HD vectors containing the affinity-enhanced Ad35^{++} fiber knob. (B) Experimental design of the study demonstrating in vivo HSPC transduction with HD-Ad vectors. hCD46tg mice were mobilized and IV injected with HD-Ad–GFP (2 injections, each 2 × 10^{10} vp) or a 1:1 mixture of HD-Ad–GFP plus HD-Ad–SB (2 injections, each 4 × 10^{10} vp). Groups of mice were euthanized at 3 days, 4, 8, 12, and 20 weeks after injection, and BM cells, splenocytes, and PBMCs were harvested. GFP expression in total MNCs (for BM, spleen, and PBMC) and BM LSK cells was analyzed by flow cytometry. (C) Mobilized and nonmobilized hCD46tg animals were injected with HD-Ad–SB + HD-Ad–GFP. BM cells (left), splenocytes (middle), and PBMCs (right) were collected 3 days after transduction, and expression of GFP in

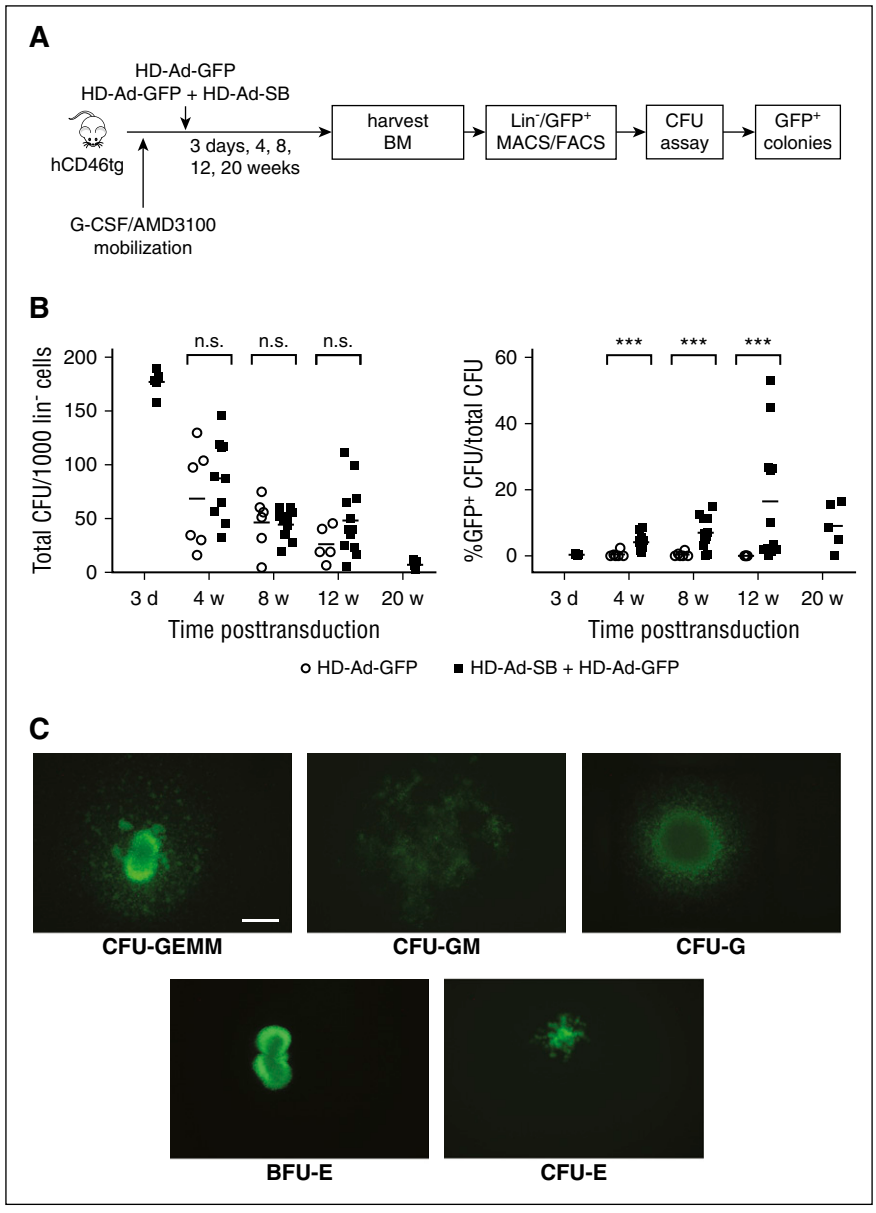

Figure 3. In vivo transduction of HSPCs with CFU potential. hCD46tg animals were mobilized and in vivo transduced with HD-Ad–GFP (n = 6 for 4 and 8 weeks, and n = 5 for 12 weeks after transduction) alone or with a combination of HD-Ad–GFP and HD-Ad–SB (n = 5 for 3 days, n = 10 for 4 weeks, n = 12 for 8 and 12 weeks, and n = 5 for 20 weeks post-transduction). Animals were euthanized 3 days, 4, 8, 12, or 20 weeks after transduction, BM cells were isolated, lineage depleted via MACS, and followed by the collection of GFP^+ cells via fluorescence-activated cell sorting. Cells were then plated in CFU assays and colonies were scored 12 days after plating. (A) Experimental design. (B) Total colonies formed per 1000 plated Lin^- cells (left) and percentage of GFP^+ colonies among total CFUs (right). Shown are single animals as well as group means. (Open circles, HD-Ad-GFP; filled squares, HD-Ad-SB + HD-Ad-GFP.) Two-way ANOVA with Bonferroni posttesting for multiple comparisons = n.s. $^{***}P < .001$. (C) GFP expression in progenitor colonies. Examples for GFP^+ erythroid burst-forming units, CFUs of erythroid progenitors (erythroid CFU), granulocyte progenitors, granulocyte/macrophage progenitors, and multipotential progenitor cells (granulocyte, erythrocyte, monocyte, and megakaryocyte CFUs) are shown. The scale bar is 500 μm. No specific feature within images shown in panel C was enhanced, obscured, moved, removed, or introduced. BFU-E, erythroid burst-forming unit; CFU-E, erythroid CFU; CFU-G, granulocyte CFU; CFU-GEMM, granulocyte, erythrocyte, monocyte, and megakaryocyte CFU; CFU-GM, granulocyte/macrophage CFU; MACS, magnetic-activated cell sorting; n.s., not significant.

(HSCs), which then give rise to transgene-expressing progeny. Moreover, no abnormalities in blood cell counts/blood chemistry and tissue histology were found in transplant recipients, suggesting the absence of oncogenic or inflammatory events (supplemental Figure 7).

Safety of IV HD-Ad5/35^{++} vector injection

Although the IV injection of first-generation Ad5/35 vectors was shown to be safe in hCD46tg mice[24] and baboons,[25] the safety of IV injections of HD-Ad5/35^{++} vectors into mobilized animals had to be shown. The bio-distribution of HD-Ad–GFP was assessed by quantitative PCR and on tissue sections at 3 days after injection into mobilized animals. Vector genomes were detected in the lung, liver, heart, kidney, and spleen at levels between 5 and 20 genome copies per cell (Figure 5A).[26-28] Vector DNA levels in the gastrointestinal tract and ovaries were 2 orders of magnitude lower. We speculate that the vector PCR signals in the lung, liver, kidney, and spleen reflect transduced leukocytes either as part of residual blood or as tissue infiltrates. This is supported by immunofluorescence studies on liver sections showing GFP expression in $CD45^+$ leukocytes (Figure 5B, middle panel). To illustrate

Figure 2 (continued) different lineages as well as LSK cells and total MNCs were analyzed via flow cytometry. N = 5. $^*P < .05$ after two-way ANOVA with Bonferroni posttesting.$^{**}P < .01$; $^{***}P < .001$; $^{****}P < .0001$. (D) GFP expression in total BM (upper left), spleen (lower left), and peripheral blood MNCs (lower right), as well as BM LSK cells (upper right). Circles represent animals injected with HD-Ad–GFP only (N = 6). Squares represent animals injected with HD-Ad–GFP + HD-Ad–SB euthanized at 3 days (N = 5), 4 (N = 10), 8 (N = 10), 12 (N = 11), and 20 weeks (N = 5) after transduction. Each data point represents a single animal. $^{**}P < .01$. (E) GFP marking in hematopoietic lineages of BM and spleen. Animals were euthanized 3 days as well as 8 and 20 weeks after transduction, and GFP expression in different lineages was analyzed via flow cytometry. Shown is the mean ± SD percentage of GFP^+ cells in the indicated lineages. $^{****}P < .0001$. Some of the data, eg, the decrease in $GFP^+/CD19^+$ cells and the increase in $GFP^+/Gr\text{-}1^+$ cells in the BM between weeks 8 and 20 cannot be readily explained. ITR, inverted terminal repeats; PGK, phosphoglycerate kinase.

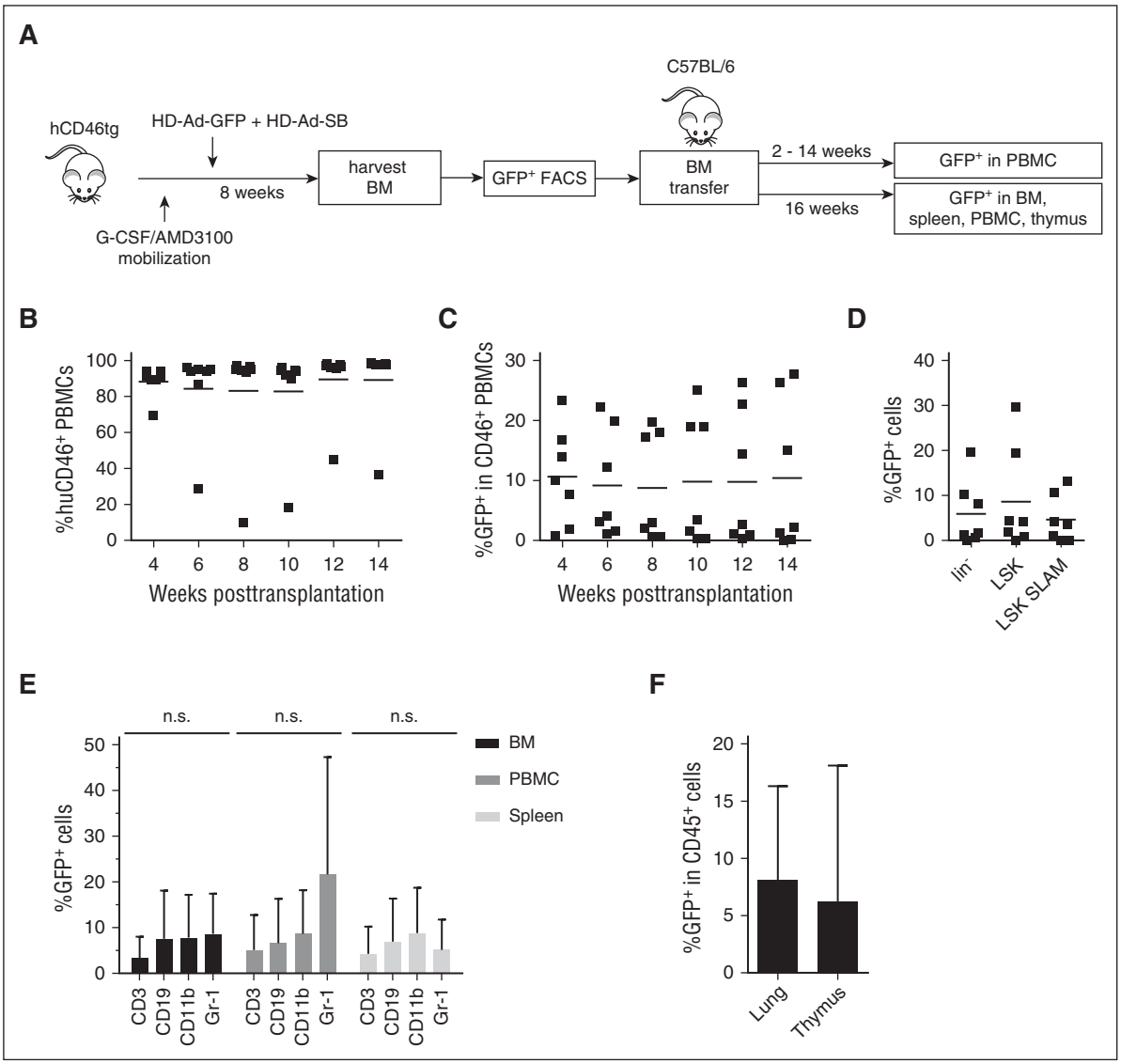

Figure 4. Gene-modified HSPCs are capable of long-term, multilineage reconstitution of lethally irradiated recipients. (A) Experimental design. BM harvested from hCD46tg mice 8 weeks after in vivo transduction with HD-Ad–GFP and HD-Ad–SB was sorted for GFP^+ cells. A total of 1×10^6 GFP^+ cells per recipient (pooled from different mice) were transplanted into lethally irradiated C57BL/6 mice. PBMCs were collected 4, 6, 8, 10, 12, and 14 weeks after transplantation, and analyzed for hCD46 and GFP expression by flow cytometry. N = 7. (B) Engraftment rate of transplanted cells based on hCD46 flow cytometry of PBMCs. Shown are single animals (filled squares) and the mean. (C) Percentage of GFP^+ PBMCs analyzed at the indicated time points. (D) Week 16 GFP marking in BM lineage-depleted cells and cell fractions enriched for HSPCs (LSK, SLAM [$LSK/CD150^+/CD48^-$]). (E) Week 16 GFP marking in BM, PBMCs, and spleen lineage-committed cells (CD3, CD19, CD11b, and Gr-1). Shown are mean ± SD. One-way ANOVA with Bonferroni posttesting. (F) GFP expression in $CD45^+$ cells of the lung and thymus. Shown are mean ± SD. n.s., not significant; SLAM, signaling lymphocyte activation molecules.

the absence of hepatocyte transduction by HD-Ad–GFP, we injected mobilized mice with a GFP-expressing Ad serotype 5 (Ad5-GFP). Three days later, the Ad5-GFP injection yielded ~50% of GFP^+ hepatocytes (Figure 5B, lower panel), whereas no hepatocyte transduction was observed with HD-Ad–GFP. In line with this, HD-Ad–GFP caused no liver toxicity (as reflected in alanine aminotransferase and aspartate aminotransferase levels) in contrast to the Ad5 vector (Figure 5C). Serum levels of cytokines IL-6, IL-10, tumor necrosis factor-α, IL-12p70, and interferon-γ were below the detection limit of the cytometric bead array used for detection (Figure 5D). Levels of the pro-inflammatory chemokine membrane cofactor protein-1 were elevated compared with untreated animals but still markedly lower than in other studies with Ad vectors,[29] most likely due to dexamethasone administration before virus injection.[30]

The genotoxic potential of SB100×-mediated transgene integration after in vivo transduction was assessed in genomic DNA isolated from GFP^+ progenitor colonies through genome-wide integration analysis using linear amplification method-PCR and next-generation sequencing. A total of 155 distinct SB100×-mediated integration sites were identified (Figures 6A-B). Integration into intergenic and intronic regions had occurred in 64% and 34% of events, respectively, whereas 1.3% of integrations were in exons (Figure 6C). No integration within or near a proto-oncogene was found (supplemental Figure 8A). The average distance to the closest cancer-related gene was 1689 kb. The level of randomness of integration was 72% without preferential integration in any given window of the whole mouse genome (supplemental Figure 8B). We have analyzed in more detail the potential integration "hotspot" on chromosome 13. None of the integrations in

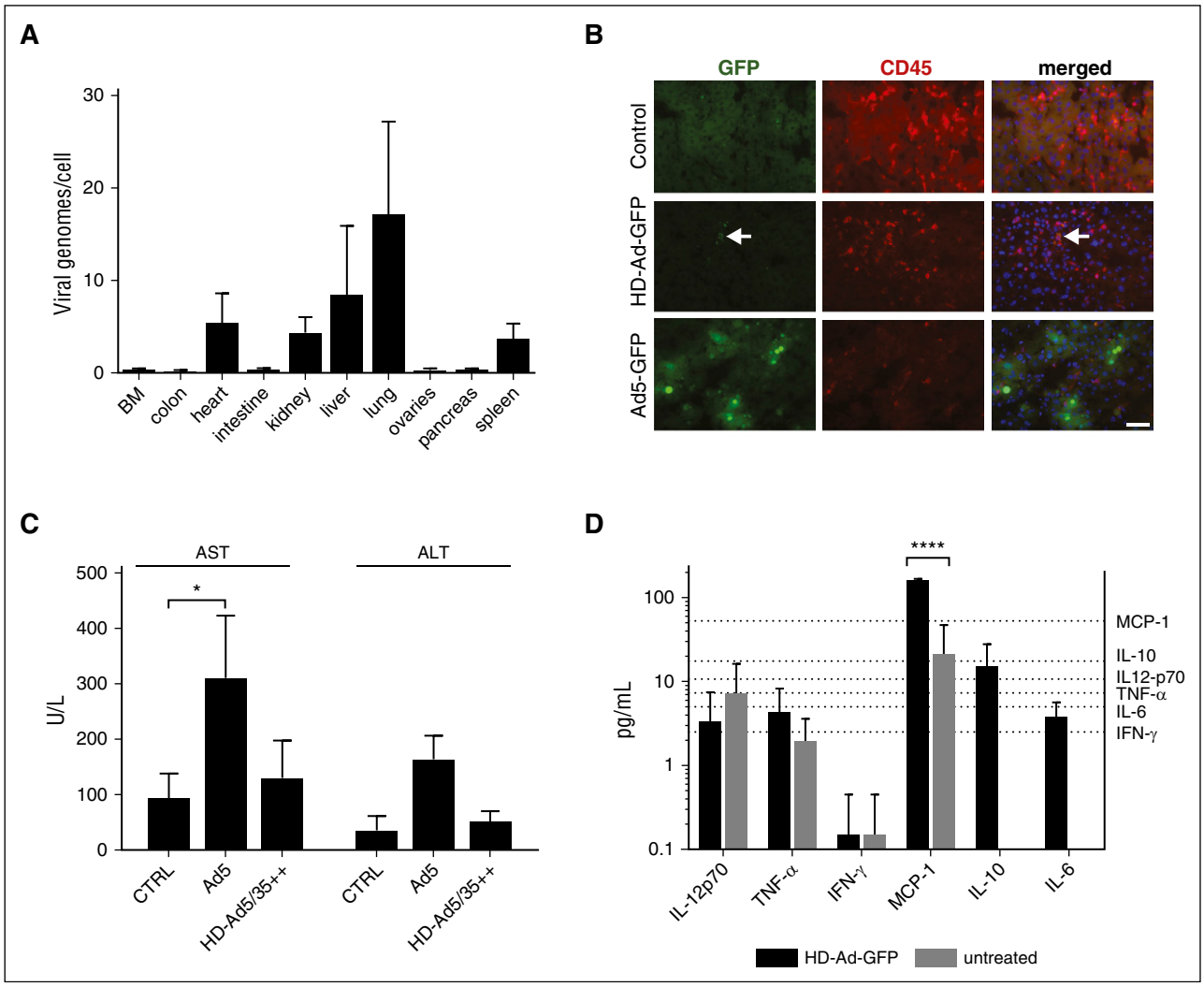

Figure 5. HD-Ad5/35 vector genome distribution and inflammatory reaction in hCD46tg mice. (A) HD-Ad–GFP (4×10^{10} vp) was IV injected into mobilized hCD46tg mice. Animals received dexamethasone (10 mg/kg) IP 16 hours and 2 hours before virus injection. Three days later, genomic DNA from tissue samples was analyzed for HD-Ad vector genomes using quantitative PCR with GFP-specific primers. Shown are vector copies per cell. N = 3. (B) Immunofluorescence analysis of liver sections at day 3 after vector injection into mobilized mice. Mice received either HD-Ad–GFP or first-generation Ad5-GFP at a dose of 4×10^{10} vp per animal. GFP appears in green, murine CD45 in red, and DAPI-stained nuclei in blue. The arrows in the middle panel indicate transduced blood cells present in a liver blood vessel. The scale bar is 50 μm. No specific feature within images shown in panel B was enhanced, obscured, moved, removed, or introduced. Previously, we and others have shown that Ad5 entry into hepatocytes is mediated by Ad5 hexon protein interaction with coagulation FX[26,27] and that this pathway is inefficient if Ad5 vectors contain the short Ad35 fibers (such as in the Ad5/35^{++} vectors used here), most likely due to a steric block of the FX-interacting domains within the Ad5 hexon.[28] (C) Levels of serum alanine transaminase and aspartate transaminase at day 3 after Ad injection. N = 3. *$P < .05$, ****$P < .0001$ after one-way ANOVA with Bonferroni posttesting. (D) Serum levels of different cytokines, 6 hours after vector injection in mobilized animals. Animals had been mobilized as before and a total of 8×10^{10} vp HD-Ad–GFP was IV injected. Shown are mean ± SD. Dotted lines represent the detection limits of the different cytokines. Serum of unmobilized, uninjected animals was used as a control (untreated). N = 5. CTRL, control; FX, factor X; IFN, interferon; MCP, membrane cofactor protein; TNF, tumor necrosis factor.

this region occurred within genes and near genes associated with cancer development.

In vivo HSPC transduction in humanized mice

The hCD46 levels in human CD34$^+$ cells were slightly increased in the more primitive CD34$^+$/CD38$^-$ subfraction (Figure 7A), However, in human PBMCs spiked with CD34$^+$ cells, no differences in CD46 levels between CD34$^+$ and CD34$^-$ cells were found (supplemental Figure 9). We first demonstrated, in vitro, in progenitor colony assays that the co-infection of human CD34$^+$ cells with HD-Ad–SB and HD-Ad–GFP resulted in stable transduction, indicating that our vector system is functional in human HSPCs (supplemental Figure 10).

To establish humanized mice, we transplanted human CD34$^+$ cells into sublethally irradiated, immunodeficient NOG mice. Average engraftment rates at 6 weeks after transplantation were 25% based on huCD45$^+$ cells in the blood. Of note, all human cells express the HD-Ad5/35^{++} receptor hCD46. G-CSF/AMD3100 mobilization led a 2.3- and 8.2-fold increase in circulating human and murine CFU, respectively, showing inferior mobilization performance compared with our hCD46tg mouse model (Figure 7B). This is most likely due to abnormal BM structure and hematopoiesis observed in NOG mice.[31] Three days after mobilization and HD-Ad–GFP + HD-Ad–SB injection, GFP expression was analyzed in the BM, spleen, and PBMCs in huCD45$^+$ cells and in more primitive subfractions (CD34$^+$ and c-Kit$^+$) (Figure 7C). In the BM, ~0.5% of huCD45$^+$ cells were GFP$^+$, whereas the GFP marking rate in the CD34$^+$ cell fraction was approximately

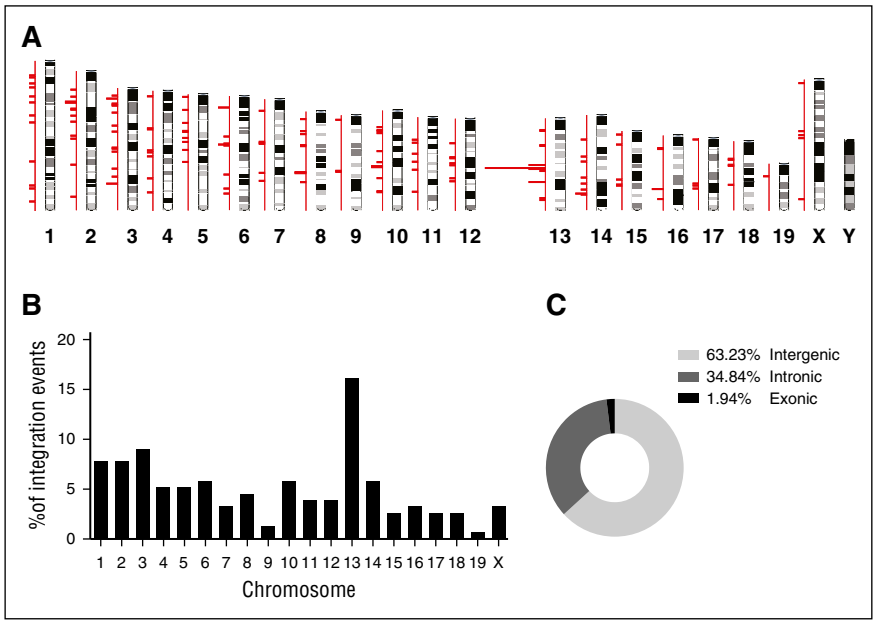

Figure 6. Analysis of vector integration sites in HSPCs. Genomic DNA isolated from 20 pooled GFP$^+$ progenitor colonies from BM cells of female hCD46tg animals, harvested 8 weeks after HD-Ad–GFP + HD-Ad–SB in vivo transduction and SB-mediated transgene integration sites were recovered. (A) Chromosomal distribution of integration sites in GFP$^+$ CFU colonies. (B) Percentage of total integration events per chromosome. (C) Integration sites were mapped to the mouse genome, and their location with respect to genes was analyzed. Shown is the percentage of integration events that occurred outside of genes, within intronic regions, and within exons, respectively.

twofold higher. This was even more pronounced in the spleen, where 43.6- and 22.3-fold more GFP$^+$/CD34$^+$ and GFP$^+$/c-Kit$^+$ cells than GFP$^+$/CD45$^+$ cells were found, respectively. To assess stable transduction and expansion of transduced cells, GFP expression in huCD45$^+$ cells was compared at day 3 and week 4 after in vivo transduction (Figure 7D). In the BM, 0.2% and 2.5% of huCD45$^+$ cells were GFP$^+$, 3 days and 4 weeks after transduction, whereas in the spleen GFP marking was 0.1% and 7.6%, respectively, showing expansion of transduced human HSPCs.

Mobilization resulted in a drastic increase in CD3$^+$ cells particularly in the BM, and to a lesser degree in the spleen and blood (Figure 7E). This can in part be explained by the fact that the lymphoid compartment in NOG mice is mostly depleted, which provides space for expansion of existing lymphoid cells. Notably, GFP marking in CD3$^+$ cells was very low (0.075%) at 3 days after transduction and decreased further by 4 weeks after transduction, possibly due to the strong expansion of CD3$^+$ cells (Figure 7F). Importantly, GFP marking in myeloid CD33$^+$ cells in the BM greatly increased (13-fold) between day 3 and week 4. Although at 3 days after transduction no GFP$^+$/CD19$^+$ cells were detected, 1.2% of CD19$^+$ cells were GFP$^+$ 4 weeks after transduction, strongly suggesting that HSPCs as well as myeloid and lymphoid progenitors had been transduced and differentiated, and expanded over time. Further studies over a longer time period are required to support this conclusion.

Discussion

Here, we demonstrate that we can stably genetically modify rare, primitive, long-term reconstituting HSPCs, a prerequisite for a long-term/life-long genetic cure of inherited and acquired diseases.[4] At week 20, we detected GFP marking in 6.4% of BM LSK cells (Figure 2D), which corresponds to ~0.05% of all total mononuclear BM cells. We did not find published data on lentivirus vector-mediated, long-term gene marking in BM HSCs in mice. In non-human primate and human studies with ex vivo lentivirus vector-transduced HSCs, it was estimated that one in 1 million transplanted HSCs were capable of long-term repopulation.[32,33] In the human trials, this would correspond to 200 to 300 gene-corrected, long-term engrafting cells per 1.5×10^{12} total MNCs in the human BM.[4] The fact that our approach allows for the transduction of primitive HSPCs and that the percentage of these cells increases over time (Figure 3B), suggests that transduced HSPCs self-renew and give rise to GFP$^+$ progeny cells that slowly overtake the BM.

Our new technology for in vivo HSPC transduction is based on a number of novel features, as shown in the sections to follow.

Mobilized HSPCs can be transduced with HD-Ad5/35^{++} vectors in the periphery, and home back to the BM and spleen

HSPCs in the BM cannot be efficiently transduced by IV injected gene transfer vectors, even if they express the targeted receptor. Limited accessibility of HSPCs and/or hCD46 due to BM stroma and inefficient virus extravasation from blood vessels could account for this. The rigidness of BM stroma and limited space in the BM also makes direct intra-osseous injection of gene transfer vectors or cells inefficient and difficult to control.[34,35] Here, we show that G-SCF/AMD3100 mobilization can circumvent these problems and allow for the transduction of mobilized HSPCs (Figures 1F and 2C). Within 2 hours after IV vector injection, ~25% of mobilized LSK cells were transduced. By day 3 after injection, no GFP$^+$ LSK cells remained in the peripheral blood; concurrently GFP-expressing LSK cells appeared in the BM and spleen.

HD-Ad5/35^{++} vectors efficiently transduce primitive HSPCs

In the BM of both the hCD46tg and NOG/hCD34$^+$ mice, transduction levels at day 3 were higher in HSPCs compared with total MNCs (Figures 1F, 2C, and 7C). In hCD46tg mice, this can be attributed to higher hCD46 levels on HSPCs (Figure 1A). Targeting of long-term surviving, multipotent HSPCs by HD-Ad5/35^{++} vectors is supported by CFU and in vivo repopulation assays (Figures 3C and 4). Compared with lentivirus and recombinant adeno-associated virus vectors, additional advantages of HD-Ad5/35^{++} vectors in HSPC gene therapy include: (1) the large transgene

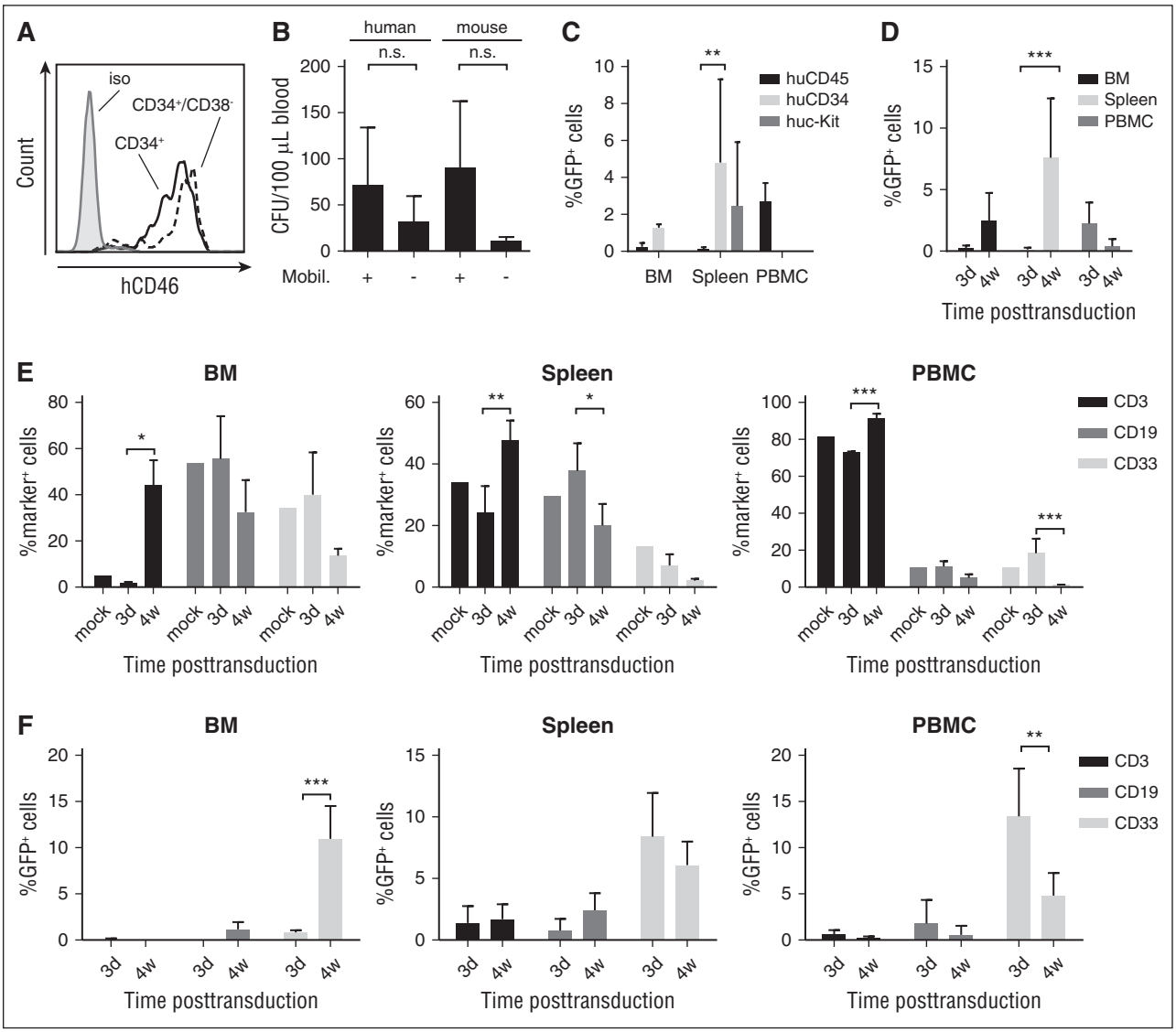

Figure 7. HSPC in vivo transduction in a humanized mouse model. (A) CD46 MFI on human CD34$^+$ and CD34$^+$/CD38$^-$ cells derived from umbilical cord blood MNCs. (B-D) In vivo studies in humanized mice. NOG mice received whole body irradiation and were transplanted with human CD34$^+$ cells. Six weeks after transplantation, successful engraftment was confirmed by huCD45 flow cytometry of PBMCs. Animals were then mobilized and injected with HD-Ad–SB + HD-Ad–GFP. (B) Mobilization of human HSPCs. PBMCs were collected 90 minutes after AMD3100. PBMCs were plated in CFU assays in the presence of human or murine cytokines. Total CFU were enumerated 12 days after plating. N = 2. Differences between mobilized and nonmobilized animals were not statistically significant after unpaired Student *t* tests. (C) GFP expression in total human CD45$^+$ cells and in HSPCs (CD34$^+$ or c-Kit$^+$ cells) in the BM, spleen, and PBMCs 3 days after HD-Ad–SB + HD-Ad–GFP injection into mobilized mice. N = 2. $^{**}P < .01$ after one-way ANOVA with Bonferroni posttesting. (D) GFP expression in human (hCD45$^+$) cells in the BM and spleen at day 3 (N = 4) and week 4 (N = 7) after in vivo transduction with HD-Ad–SB + HD-Ad–GFP. Values represent mean ± SD. $^{***}P < .001$ after one-way ANOVA with Bonferroni posttesting. (E-F) Lineage composition of hematopoietic tissues and transgene expression in hematopoietic lineages following HSPC in vivo transduction. Humanized NOG mice were mobilized and injected with HD-Ad–SB + HD-Ad–GFP as before. Animals were euthanized at 3 days (n = 2) or 4 weeks (n = 3) after transduction, and expression of GFP and lineage surface markers was assessed via flow cytometry. (E) Expression of hematopoietic lineage surface markers after HSPC in vivo transduction in the BM, spleen, and peripheral blood. An unmobilized, untreated, humanized NOG animal was used as control (mock). Shown are mean ± SD. (F) GFP expression in hematopoietic lineages at 3 days and 4 weeks after HSPC in vivo transduction. Shown are mean ± SD. $^*P < .05$ following two-way ANOVA with Bonferroni posttesting. $^{**}P < .01$; $^{***}P < .001$. iso, isolated; n.s., not significant; mobil, mobilized.

insert capacity (30 kb); (2) no requirement for cell cycling[7]; and (3) the relatively low manufacturing costs.

HD-Ad5/35^{++} vectors encoding SB transposase allow for transgene integration in HSPCs

A major advantage of the SB100× integration system is its independence of the cellular DNA repair and recombination machinery, the low activity of which in HSPCs (which are, per se, quiescent), limits other integration strategies involving nonhomologous end joining or homologous recombination.[36] In contrast to lentiviral[37] or adeno-associated virus vectors,[38] SB100×-mediated integration is not biased toward insertion into or near genes,[12] leading to a lower risk of genotoxic events. GFP marking rates with the HD-Ad5/35^{++}-based SB100× system varied between individual animals. We excluded that these differences were due to inefficient HSPC mobilization in a subset of mice. The numbers of CFU in the blood 2 hours after AMD3100 were comparable between individual mice (data not shown). Furthermore, GFP marking analyzed at day 3 did not show dramatic differences between animals. A potential explanation for

the variations in GFP marking in individual animals at week 8 and 20 could be related to the fact that true HSPCs are rare, and might not have been transduced in all animals. Also, the impact of anti-GFP immune responses on GFP marking in the BM could be considered.

IV injection of HD-Ad5/35^{++} vectors into mobilized hCD46tg mice was safe

Our studies in mobilized hCD46tg mice demonstrate that IV injection of HD-Ad5/35^{++} vectors was well tolerated. Ongoing studies in non-human primates corroborate this conclusion.

Innate acute toxicity is a major problem of systemic administration of Ad5-based vectors in animals and humans.[39-41] Previous studies showed that release and expression of pro-inflammatory cytokines associated with vector uptake by the reticulo-endothelial system of the liver and spleen were markedly lower after IV injection of Ad5/35 vectors than after Ad5 vectors.[24,25,42-44] Furthermore, in contrast to Ad5 vectors, our HD-Ad5/35^{++} vectors do not transduce hepatocytes after IV injection (Figure 5B), which is in agreement with previous Ad5/35 vector studies in hCD46tg mice and non-human primates.[24,25,45,46] HD-Ad5/35^{++} vectors not only transduced mobilized HSPCs but also other differentiated peripheral blood and mobilized cells after IV injection (Figure 2C). However, because of the limited lifespan of differentiated blood cells, their genetic modification will not critically affect the safety of our approach. At day 3 after injection, vector genomes detected in tissues were mostly associated with transduced blood cells. Importantly, no GFP^{+} cells were found in germ line tissues, suggesting that low hCD46 levels and/or lack of accessibility of hCD46 to IV injected virus vector on nonhematopoietic tissues prevented their efficient transduction. A problem we encountered in our study was the development of anti-GFP immune responses that most likely resulted in the elimination of GFP-expressing PBMCs. Earlier studies involving the transplantation of retrovirus-transduced HSPCs also associated the loss of GFP marking in the periphery with anti-GFP T-cell responses.[47-50] This problem can be addressed by immuno-modulation[51] or -suppression[47] approaches.

Our data provide a basis for future studies in animal disease models, aimed at assessing the therapeutic potential of our approach. The simplicity and cost-effectiveness of the technology is relevant for gene therapy of inherited or infectious diseases, and cancer.[52,53]

Acknowledgments

The authors thank Pavel Sova for help with the integration site analysis; and Stanley Riddell and Ashwini Balakrishnan (Fred Hutchinson Cancer Research Center) for support in the T-cell assays.

The study was supported by grants from the National Institutes of Health, National Cancer Institute (R21 CA193077) and the National Heart, Lung, and Blood Institute (R01HL128288), a grant from the "Wings of Karen" Foundation, and a grant from the University of Washington CoMotion Innovation Fund (A.L.). M.R. was supported through a scholarship from the German Academic Exchange Service. J.L. was supported through a scholarship of the Chinese Scholarship Council. No specific feature within images shown in Figures 3C and 5B, and supplemental Figures 2C and 4 were enhanced, obscured, moved, removed, or introduced.

Authorship

Contribution: A.L. provided the conceptual framework for the study; M.R., T.P., Z.I., A.E., and P.N. designed the experiments; M.R., K.S., R.Y., R.K., J.L., E.-E.N., M.S., D.P., P.N., and K.G.H. performed the experiments; R.C. provided critical material; Z.I., W.U., P.N., A.E., T.P., and H.-P.K. provided comments; and M.R. and A.L. wrote the manuscript.

Conflict-of-interest disclosure: The authors declare no competing financial interests.

Correspondence: André Lieber, Department of Medicine, Division of Medical Genetics, University of Washington, Seattle, WA 98195; e-mail: lieber00@uw.edu.

References

1. Naldini L. Gene therapy returns to centre stage. *Nature.* 2015;526(7573):351-360.
2. Bonig H, Papayannopoulou T. Mobilization of hematopoietic stem/progenitor cells: general principles and molecular mechanisms. *Methods Mol Biol.* 2012;904:1-14.
3. Fruehauf S, Veldwijk MR, Seeger T, et al. A combination of granulocyte-colony-stimulating factor (G-CSF) and plerixafor mobilizes more primitive peripheral blood progenitor cells than G-CSF alone: results of a European phase II study. *Cytotherapy.* 2009;11(8):992-1001.
4. Abkowitz JL, Catlin SN, McCallie MT, Guttorp P. Evidence that the number of hematopoietic stem cells per animal is conserved in mammals. *Blood.* 2002;100(7):2665-2667.
5. Li L, Krymskaya L, Wang J, et al. Genomic editing of the HIV-1 coreceptor CCR5 in adult hematopoietic stem and progenitor cells using zinc finger nucleases. *Mol Ther.* 2013;21(6):1259-1269.
6. Gaggar A, Shayakhmetov DM, Lieber A. CD46 is a cellular receptor for group B adenoviruses. *Nat Med.* 2003;9(11):1408-1412.
7. Nilsson M, Karlsson S, Fan X. Functionally distinct subpopulations of cord blood CD34+ cells are transduced by adenoviral vectors with serotype 5 or 35 tropism. *Mol Ther.* 2004;9(3):377-388.
8. Shayakhmetov DM, Papayannopoulou T, Stamatoyannopoulos G, Lieber A. Efficient gene transfer into human CD34(+) cells by a retargeted adenovirus vector. *J Virol.* 2000;74(6):2567-2583.
9. Yotnda P, Onishi H, Heslop HE, et al. Efficient infection of primitive hematopoietic stem cells by modified adenovirus. *Gene Ther.* 2001;8(12):930-937.
10. Tuve S, Wang H, Ware C, et al. A new group B adenovirus receptor is expressed at high levels on human stem and tumor cells. *J Virol.* 2006;80(24):12109-12120.
11. Wang H, Liu Y, Li Z, et al. In vitro and in vivo properties of adenovirus vectors with increased affinity to CD46. *J Virol.* 2008;82(21):10567-10579.
12. Zhang W, Muck-Hausl M, Wang J, et al. Integration profile and safety of an adenovirus hybrid-vector utilizing hyperactive sleeping beauty transposase for somatic integration [published correction appears in *PLos One.* 2014;9(9):e108836]. *PLoS One.* 2013;8(10):e75344.
13. Mück-Häusl M, Solanki M, Zhang W, Ruzsics Z, Ehrhardt A. Ad 2.0: a novel recombineering platform for high-throughput generation of tailored adenoviruses. *Nucleic Acids Res.* 2015;43(8):e50.
14. Moldt B, Miskey C, Staunstrup NH, et al. Comparative genomic integration profiling of Sleeping Beauty transposons mobilized with high efficacy from integrase-defective lentiviral vectors in primary human cells. *Mol Ther.* 2011;19(8):1499-1510.
15. Kemper C, Leung M, Stephensen CB, et al. Membrane cofactor protein (MCP; CD46) expression in transgenic mice. *Clin Exp Immunol.* 2001;124(2):180-189.
16. Wilson A, Trumpp A. Bone-marrow haematopoietic-stem-cell niches. *Nat Rev Immunol.* 2006;6(2):93-106.
17. Wang H, Cao H, Wohlfahrt M, Kiem HP, Lieber A. Tightly regulated gene expression in human hematopoietic stem cells after transduction with helper-dependent Ad5/35 vectors. *Exp Hematol.* 2008;36(7):823-831.
18. Mátés L, Chuah MK, Belay E, et al. Molecular evolution of a novel hyperactive Sleeping Beauty transposase enables robust stable gene transfer in vertebrates. *Nat Genet.* 2009;41(6):753-761.
19. Morrison SJ, Weissman IL. The long-term repopulating subset of hematopoietic stem cells

is deterministic and isolatable by phenotype. *Immunity.* 1994;1(8):661-673.

20. Wang H, Shayakhmetov DM, Leege T, et al. A capsid-modified helper-dependent adenovirus vector containing the beta-globin locus control region displays a nonrandom integration pattern and allows stable, erythroid-specific gene expression. *J Virol.* 2005;79(17):10999-11013.
21. Bradford GB, Williams B, Rossi R, Bertoncello I. Quiescence, cycling, and turnover in the primitive hematopoietic stem cell compartment. *Exp Hematol.* 1997;25(5):445-453.
22. Macallan DC, Wallace DL, Zhang Y, et al. B-cell kinetics in humans: rapid turnover of peripheral blood memory cells. *Blood.* 2005;105(9): 3633-3640.
23. Kim MJ, Kim MH, Kim SA, Chang JS. Age-related deterioration of hematopoietic stem cells. *Int J Stem Cells.* 2008;1(1):55-63.
24. Ni S, Gaggar A, Di Paolo N, et al. Evaluation of adenovirus vectors containing serotype 35 fibers for tumor targeting. *Cancer Gene Ther.* 2006; 13(12):1072-1081.
25. Ni S, Bernt K, Gaggar A, Li ZY, Kiem HP, Lieber A. Evaluation of biodistribution and safety of adenovirus vectors containing group B fibers after intravenous injection into baboons. *Hum Gene Ther.* 2005;16(6):664-677.
26. Shayakhmetov DM, Gaggar A, Ni S, Li ZY, Lieber A. Adenovirus binding to blood factors results in liver cell infection and hepatotoxicity. *J Virol.* 2005;79(12):7478-7491.
27. Waddington SN, McVey JH, Bhella D, et al. Adenovirus serotype 5 hexon mediates liver gene transfer. *Cell.* 2008;132(3):397-409.
28. Liu Y, Wang H, Yumul R, et al. Transduction of liver metastases after intravenous injection of Ad5/35 or Ad35 vectors with and without factor X-binding protein pretreatment. *Hum Gene Ther.* 2009;20(6):621-629.
29. Stone D, Liu Y, Li ZY, Tuve S, Strauss R, Lieber A. Comparison of adenoviruses from species B, C, E, and F after intravenous delivery. *Mol Ther.* 2007;15(12):2146-2153.
30. Seregin SS, Appledorn DM, McBride AJ, et al. Transient pretreatment with glucocorticoid ablates innate toxicity of systemically delivered adenoviral vectors without reducing efficacy. *Mol Ther.* 2009; 17(4):685-696.
31. Kallinikou K, Anjos-Afonso F, Blundell MP, et al. Engraftment defect of cytokine-cultured adult human mobilized CD34(+) cells is related to reduced adhesion to bone marrow niche elements. *Br J Haematol.* 2012;158(6):778-787.
32. Kim S, Kim N, Presson AP, et al. Dynamics of HSPC repopulation in nonhuman primates revealed by a decade-long clonal-tracking study. *Cell Stem Cell.* 2014;14(4):473-485.
33. Biasco L, Pellin D, Scala S, et al. In vivo tracking of human hematopoiesis reveals patterns of clonal dynamics during early and steady-state reconstitution phases. *Cell Stem Cell.* 2016;19(1): 107-119.
34. Wang X, Shin SC, Chiang AF, et al. Intraosseous delivery of lentiviral vectors targeting factor VIII expression in platelets corrects murine hemophilia A. *Mol Ther.* 2015;23(4):617-626.
35. Abed S, Tubsuwan A, Chaichompoo P, et al. Transplantation of Macaca cynomolgus iPS-derived hematopoietic cells in NSG immunodeficient mice. *Haematologica.* 2015;100(10):e428-e431.
36. Beerman I, Seita J, Inlay MA, Weissman IL, Rossi DJ. Quiescent hematopoietic stem cells accumulate DNA damage during aging that is repaired upon entry into cell cycle. *Cell Stem Cell.* 2014;15(1):37-50.
37. Schröder AR, Shinn P, Chen H, Berry C, Ecker JR, Bushman F. HIV-1 integration in the human genome favors active genes and local hotspots. *Cell.* 2002;110(4):521-529.
38. Nakai H, Wu X, Fuess S, et al. Large-scale molecular characterization of adeno-associated virus vector integration in mouse liver. *J Virol.* 2005;79(6):3606-3614.
39. Brunetti-Pierri N, Palmer DJ, Beaudet AL, Carey KD, Finegold M, Ng P. Acute toxicity after high-dose systemic injection of helper-dependent adenoviral vectors into nonhuman primates. *Hum Gene Ther.* 2004;15(1):35-46.
40. Lieber A, He CY, Meuse L, et al. The role of Kupffer cell activation and viral gene expression in early liver toxicity after infusion of recombinant adenovirus vectors. *J Virol.* 1997;71(11): 8798-8807.
41. Raper SE, Chirmule N, Lee FS, et al. Fatal systemic inflammatory response syndrome in a ornithine transcarbamylase deficient patient following adenoviral gene transfer. *Mol Genet Metab.* 2003;80(1-2):148-158.
42. Di Paolo NC, Baldwin LK, Irons EE, Papayannopoulou T, Tomlinson S, Shayakhmetov DM. IL-1α and complement cooperate in triggering local neutrophilic inflammation in response to adenovirus and eliminating virus-containing cells. *PLoS Pathog.* 2014;10(3):e1004035.
43. Bernt KM, Ni S, Gaggar A, Li ZY, Shayakhmetov DM, Lieber A. The effect of sequestration by nontarget tissues on anti-tumor efficacy of systemically applied, conditionally replicating adenovirus vectors [published correction appears in *Mol Ther.* 2004;9(1):139]. *Mol Ther.* 2003;8(5): 746-755.
44. Sakurai F, Nakashima K, Yamaguchi T, et al. Adenovirus serotype 35 vector-induced innate immune responses in dendritic cells derived from wild-type and human CD46-transgenic mice: comparison with a fiber-substituted Ad vector containing fiber proteins of Ad serotype 35. *J Control Release.* 2010;148(2):212-218.
45. Sakurai F, Kawabata K, Koizumi N, et al. Adenovirus serotype 35 vector-mediated transduction into human CD46-transgenic mice. *Gene Ther.* 2006;13(14):1118-1126.
46. Sakurai F, Nakamura S, Akitomo K, et al. Transduction properties of adenovirus serotype 35 vectors after intravenous administration into nonhuman primates. *Mol Ther.* 2008;16(4): 726-733.
47. Beagles KE, Peterson L, Zhang X, Morris J, Kiem HP. Cyclosporine inhibits the development of green fluorescent protein (GFP)-specific immune responses after transplantation of GFP-expressing hematopoietic repopulating cells in dogs. *Hum Gene Ther.* 2005;16(6):725-733.
48. Morris JC, Conerly M, Thomasson B, Storek J, Riddell SR, Kiem HP. Induction of cytotoxic T-lymphocyte responses to enhanced green and yellow fluorescent proteins after myeloablative conditioning. *Blood.* 2004;103(2):492-499.
49. Stripecke R, Carmen Villacres M, Skelton D, Satake N, Halene S, Kohn D. Immune response to green fluorescent protein: implications for gene therapy. *Gene Ther.* 1999;6(7):1305-1312.
50. Rosenzweig M, Connole M, Glickman R, et al. Induction of cytotoxic T lymphocyte and antibody responses to enhanced green fluorescent protein following transplantation of transduced CD34(+) hematopoietic cells. *Blood.* 2001;97(7): 1951-1959.
51. Kay MA, Meuse L, Gown AM, et al. Transient immunomodulation with anti-CD40 ligand antibody and CTLA4Ig enhances persistence and secondary adenovirus-mediated gene transfer into mouse liver. *Proc Natl Acad Sci USA.* 1997;94(9):4686-4691.
52. Gschweng E, De Oliveira S, Kohn DB. Hematopoietic stem cells for cancer immunotherapy. *Immunol Rev.* 2014;257(1): 237-249.
53. Holt N, Wang J, Kim K, et al. Human hematopoietic stem/progenitor cells modified by zinc-finger nucleases targeted to CCR5 control HIV-1 in vivo. *Nat Biotechnol.* 2010;28(8): 839-847.

2016 128: 2206-2217
doi:10.1182/blood-2016-04-711580 originally published online August 23, 2016

In vivo transduction of primitive mobilized hematopoietic stem cells after intravenous injection of integrating adenovirus vectors

Maximilian Richter, Kamola Saydaminova, Roma Yumul, Rohini Krishnan, Jing Liu, Eniko-Eva Nagy, Manvendra Singh, Zsuzsanna Izsvák, Roberto Cattaneo, Wolfgang Uckert, Donna Palmer, Philip Ng, Kevin G. Haworth, Hans-Peter Kiem, Anja Ehrhardt, Thalia Papayannopoulou and André Lieber

Blood (print ISSN 0006-4971, online ISSN 1528-0020), is published weekly by the American Society of Hematology, 2021 L St, NW, Suite 900, Washington DC 20036.

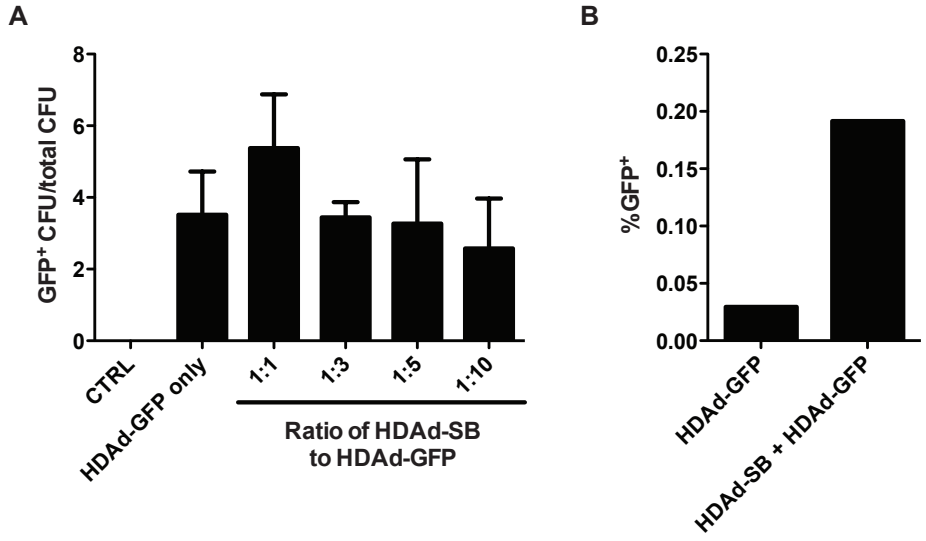

Fig.S1. Assessment of SB vector system functionality in hCD46tg mouse lin$^-$ cells in vitro. Cells were infected with HDAd-GFP alone (2000 vp/cells) or HDAd-SB + HDAd-GFP at the indicated ratios (based on an MOI of 2000 vp/cell of HDAd-GFP) and subjected to CFU assays. **A)** The study shows that a 1:1 ratio of HDAd-SB and HDAd-GFP resulted in more efficient stable transduction of lin$^-$ cells than a 1:3 ratio, a ratio that had been found to be optimal for hepatocyte transduction with HDAd vectors based on serotype 5. **B)** Lin$^-$ cells were infected with HDAd-GFP alone (MOI 2000) or HDAd-GFP (MOI 1000) plus HDAd-SB (MOI 1000) and the percentage of GFP+ cells in all cells from progenitor colonies harvested at day 12 after plating was analyzed via flow cytometry.

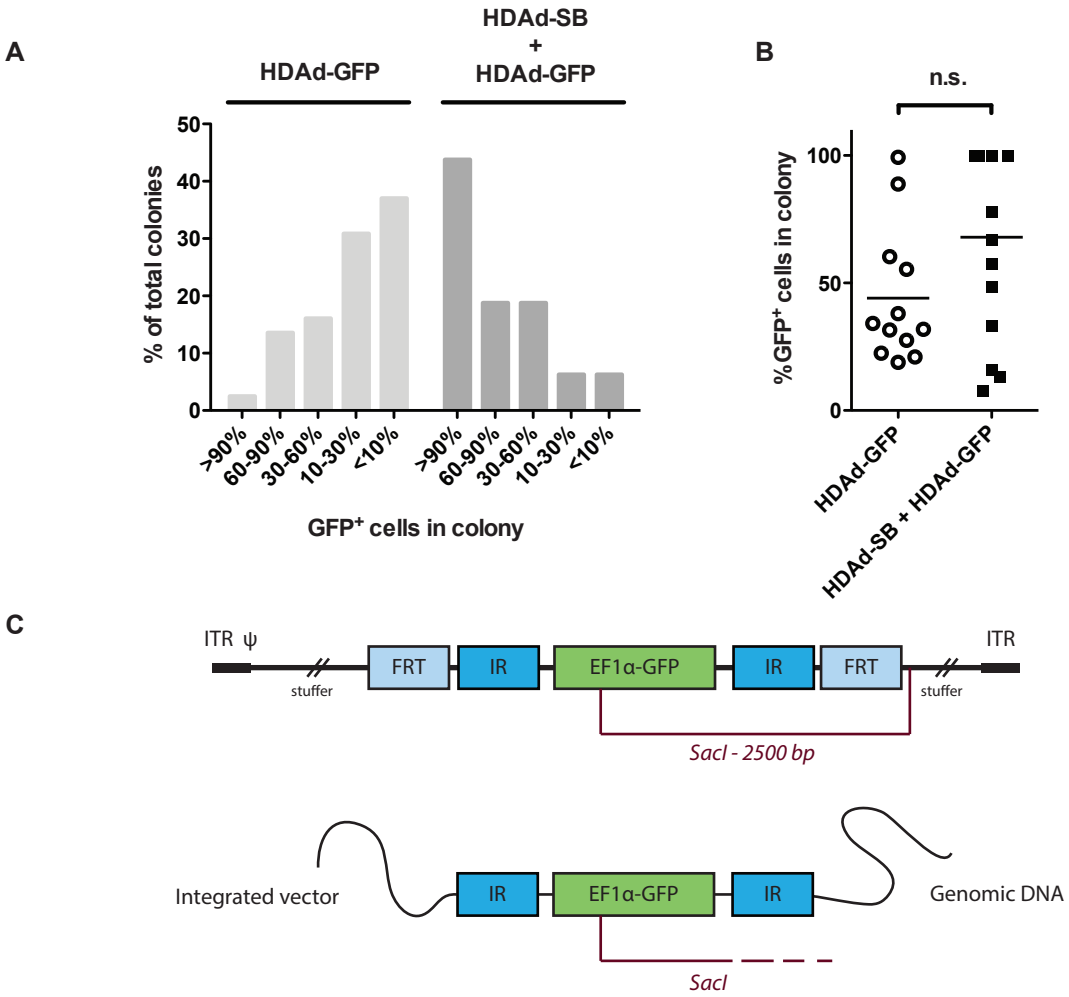

Fig.S2. Transgene integration after transduction of MO7e cells with HDAd-SB + HDAd-GFP. A-B) GFP expression in MO7e clones. MO7e cells were infected either with HDAd-GFP alone or with a 1:1 mixture of HDAd-SB and HDAd-GFP. Cells were cultured for 48 h to allow for transgene expression. GFP$^+$ cells were sorted into 96-well plates using FACS at 1 cell per well. The single clones were expanded for 2 weeks and the percentage of GFP$^+$ cells per colony was assessed visually using a UV microscope. **A)** Shown is the distribution of GFP expression for all GFP-positive colonies. Upon expansion of single transduced cells to about 10^6 cells, more than 40% of MO7e clones were found to be stably transduced with HDAd-SB plus HDAd-GFP, whereas stable transduction was less than 2% in cells infected with HDAd-GFP alone. **B)** Colonies exhibiting the highest expression levels of GFP (>30%) were further expanded. After expansion the level of GFP expression was analyzed via flow cytometry. Shown are the percentages of GFP-positive cells for single colonies as well as the mean. An unpaired T-test was performed to test for statistical significance. **C-D)** Clones with the highest expression levels of GFP were selected and further expanded for integration analysis by Southern Blot. **C)** *SacI* restriction sites in the HDAd-GFP vector genome are indicated. *SacI* digestion of non-integrated vector DNA would result in a 2500 bp restriction fragment. Sleeping Beauty-mediated integration of the GFP transposon results in SacI fragments of different lengths. **D)** Southern blot analysis of *SacI*-digested genomic DNA from MO7e clones transduced with HDAd-SB + HDAd-GFP using a GFP-specific probe. Each lane represents an individual clone. Fragments of various lengths, indicating integration into different genomic sites, are marked.

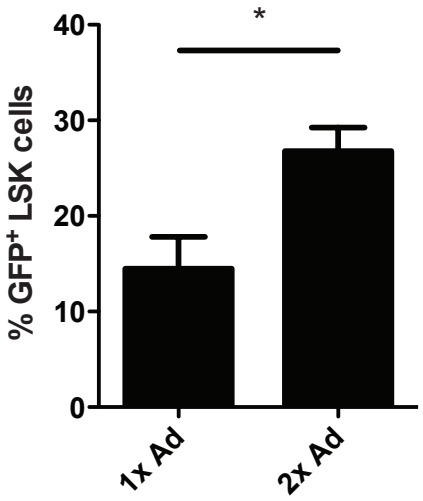

Fig.S3. Effect of increased HDAd-GFP dose on *in vivo* HSPC transduction. $2x10^{10}$ vp of HDAd-GFP was injected once at 40 min after AMD3100 (1xAd) or twice at 30 and 60 min after AMD3100 (2xAd). Shown is the percentage of GFP^+ LSK cells in PBMCs harvested two hours after Ad injection. * $p<0.05$

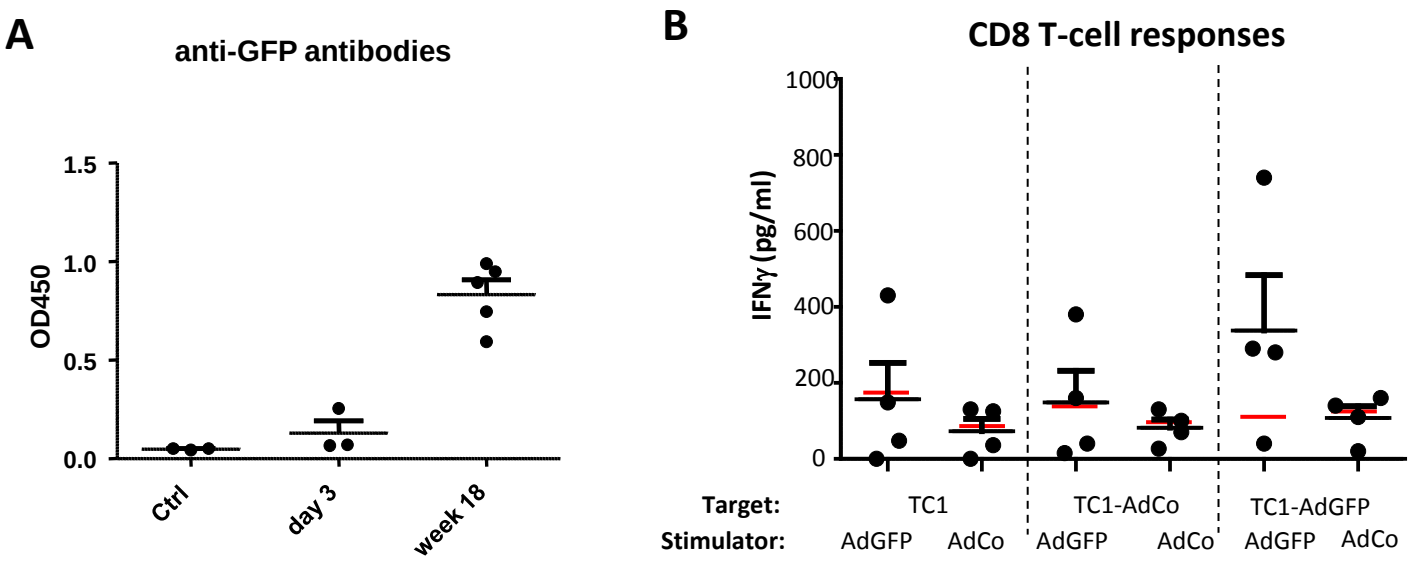

Fig.S4. Anti-GFP immune responses. **A)** Serum anti-GFP antibodies. IgG antibodies against recombinant GFP were analyzed in serum of non-transduced mice and serum from mice 3 days and 18 weeks after in vivo HSC transduction with HDAd5/35++ vectors. **B)** CD8 T-cell responses in splenocytes harvested from mice 20 weeks after *in vivo* HSC transduction. For in vitro stimulation, splenocytes from naïve hCD46 transgenic mice (C57Bl/6 background) were transduced with HDAd-GFP (AdGFP) or an HD-Ad control (AdCo) virus (without GFP) at an MOI of 1000 vp/cell, or mock-transdcued, and cultured for three days. For the T-cell assay, cells were irradiated at 2500 Rad. Splenocytes from *in vivo* transduced mice (N=4) and one naïve mouse were harvested 20 weeks after transduction. CD8 cells were isolated using the Miltenyi MACS isolation kit. These cells were mixed with stimulator cells at a ratio of 5:1 and incubated for 5 days in the presence of 10U/ml IL-2. To measure GFP-specific T-cell activation (IFNγ production), C57Bl/6 derived TC1 cancer cells were transduced with HDAd-GFP or HDAd-Co and incubated for 3 days (designated "TC1-AdCo" and "TC1-AdGFP" target cells in the figure). Target cells were incubated with *in vitro* stimulated CD8 cells at a ratio of 1:1 and IFNγ levels in the supernatants were measured by ELISA (eBioscience) 24 hours later. The red line in the figure are T-cell responses from naïve mice that were not *in vivo* transduced and most likely represent background responses to neo-antigens on TC1 tumor cells. The only significant ($p<0.05$) elevation in IFNγ levels over these background levels was seen in the setting with AdGFP stimulated cells on GFP-expressing TC1 target cells, indicating CD8 T-cell responses against GFP.

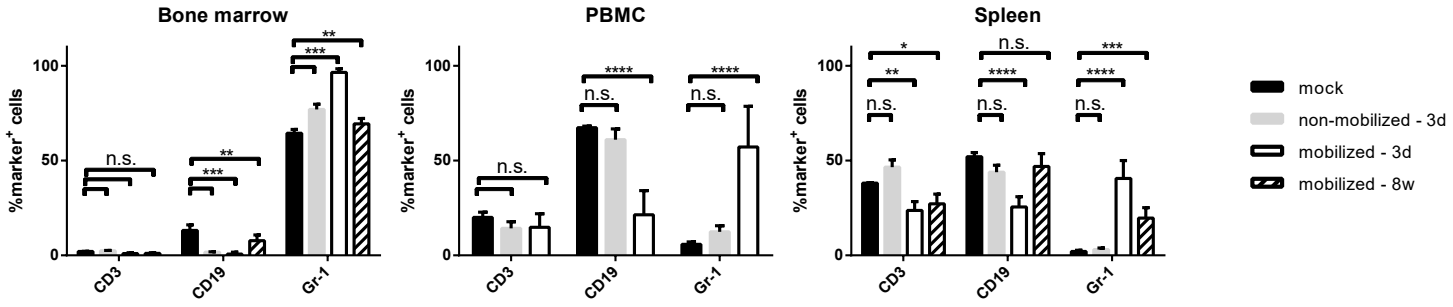

Figure S5. Effect of mobilization and HDAd5/35++ transduction on hematopoietic lineage composition of bone marrow, spleen, and peripheral blood. hCD46tg animals were mobilized and transduced with HDAd-GFP + HDAd-SB as before. Animals were sacrificed at 3 days and 8 weeks after transduction and the expression of lineage surface antigens in the bone marrow, spleen and PBMCs was analyzed via flow cytometry. As controls, unmobilized, uninjected animals (mock), as well as non-mobilized animals transduced with HDAd-GFP + HDAd-SB, sacrificed at day 3 after transduction, were used. Shown are mean ± SD. n.s. not statistically significant after two-way ANOVA with Bonferroni post testing, comparing treated animals to mock control. * $p<0.05$, ** $p<0.01$, *** $p<0.001$, **** $p<0.0001$.

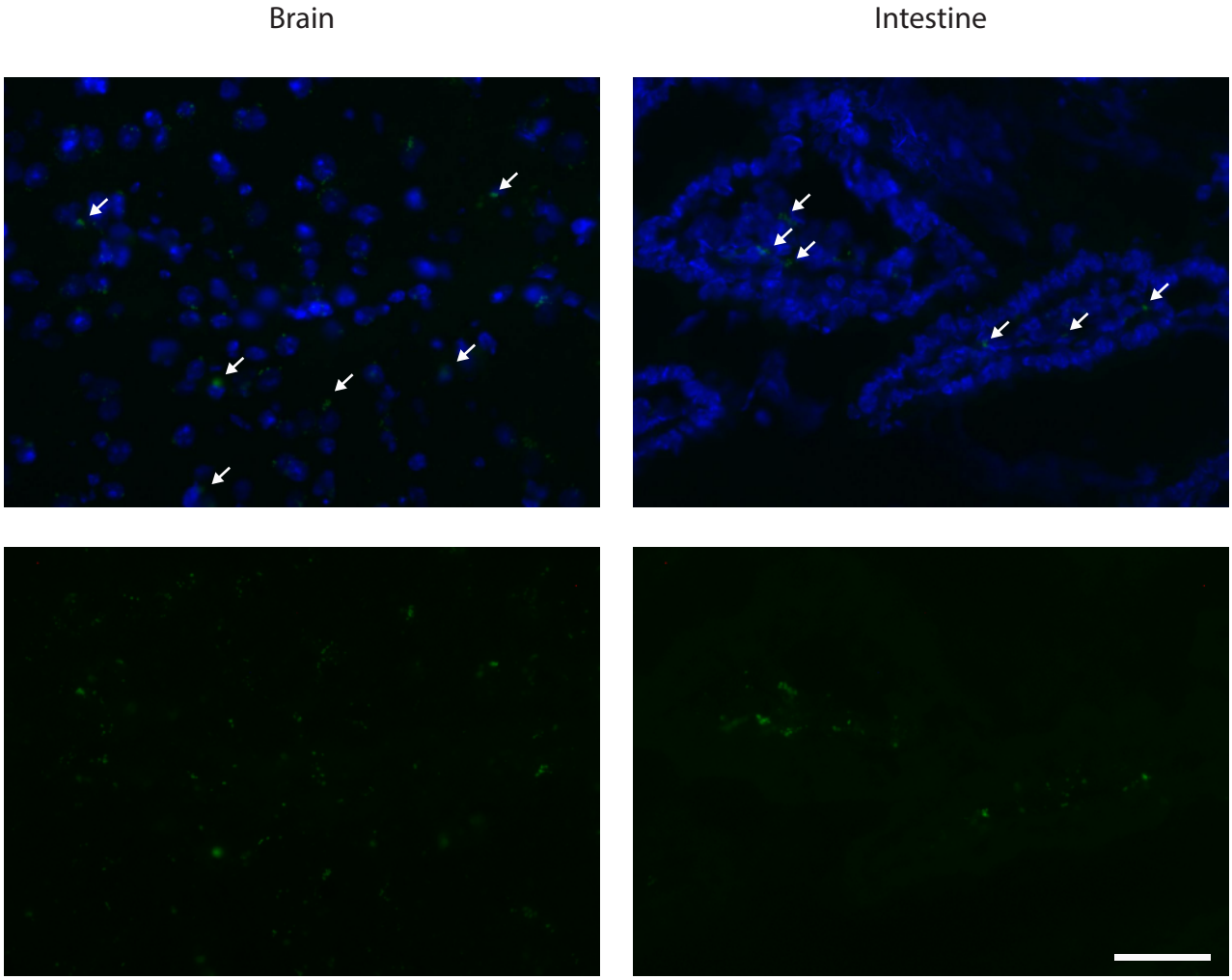

Fig.S6. Immunofluorescence analysis on sections of brain and small intestine from transplanted animals 16 weeks after transplantation. The experimental conditions are described in Fig.4. The upper panel shows the merged GFP (green) and DAPI (blue) channels. GFP^+ cells are indicated by arrows. The lower panels show GFP only. The scale bar is 50 μm.

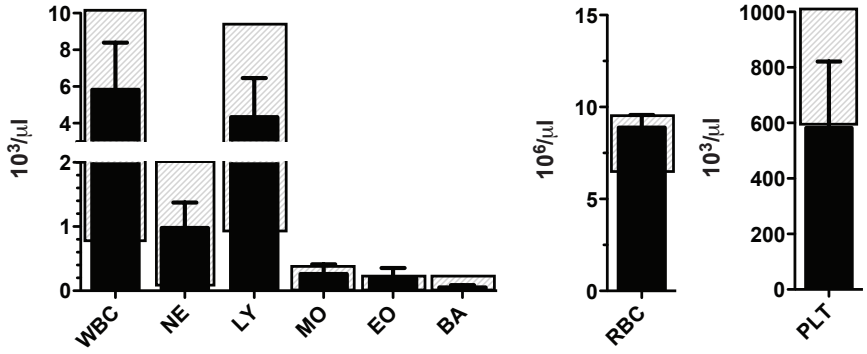

Fig.S7. Blood cell counts of transplanted animals 16 weeks after transplantation. Shown are the counts/µl for white blood cells (WBC), neutrophils (NE), lymphocytes (LY), monocytes (MO), eosinophiles (EO), basophiles (BA), red blood cells (RBC) and platelets (PLT). Shown are means ± SD. Grey boxes indicated normal ranges. N=7.

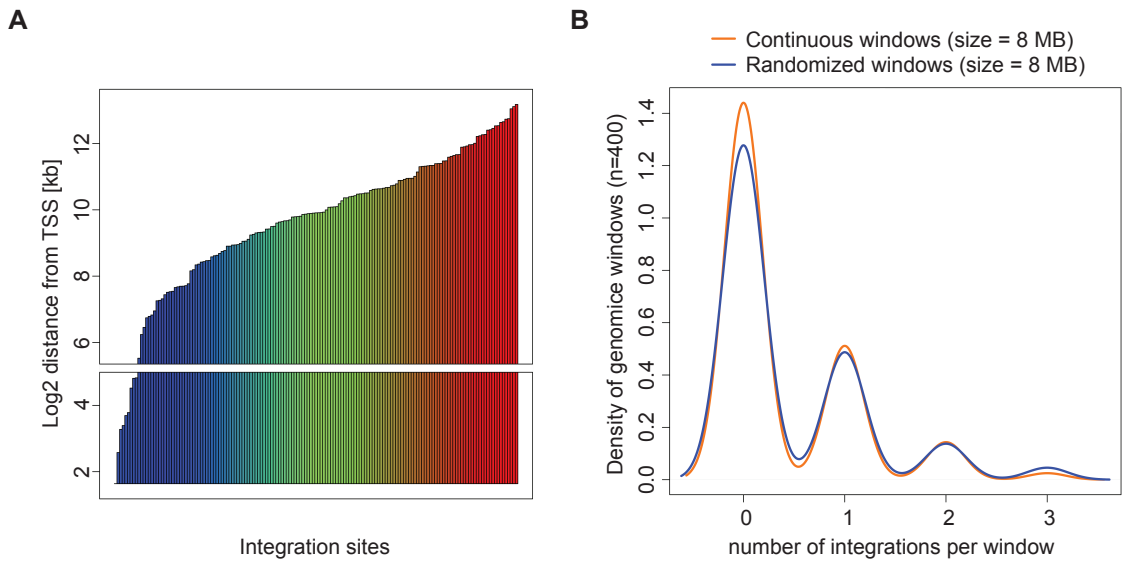

Fig. S8. Analysis of vector integration sites in HSPCs. A) Log-scaled distance (in kb) of each integration site from closest genes of KEGG pathways in cancer. The distance is shown in a color gradient, with blue being the smallest distance. **B)** Integration pattern in mouse genomic windows. The number of integrations overlapping with continuous genomic windows and randomized mouse genomic windows and size was compared. This shows that the pattern of integration is similar in continuous and random windows. Maximum number of integrations in any given window was not more than 3; with one integration per window having the higher incidence.

f

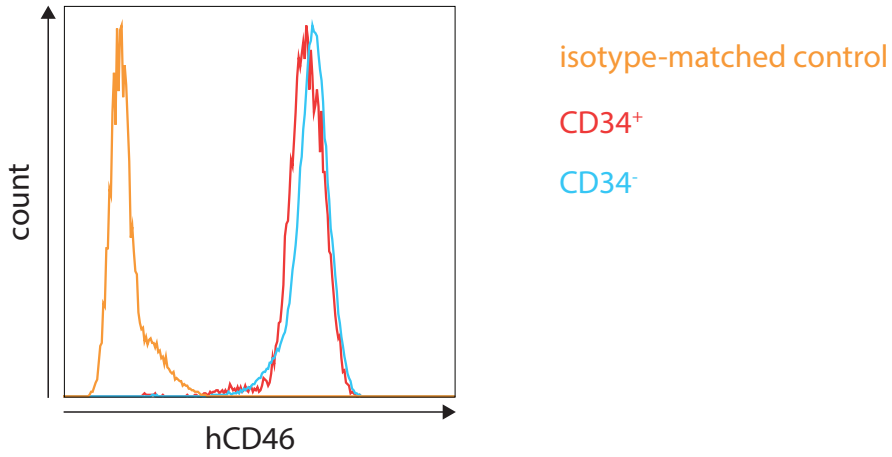

Fig.S9. CD46 expression on human hematopoietic cells. Human PBMCs were spiked with humam CD34+ cells and CD46 expression was assessed in CD34-positive (red) and CD34-negative (blue) cells via flow cytometry. An isotype-matched control (orange) was used to ensure specificity of the stain.

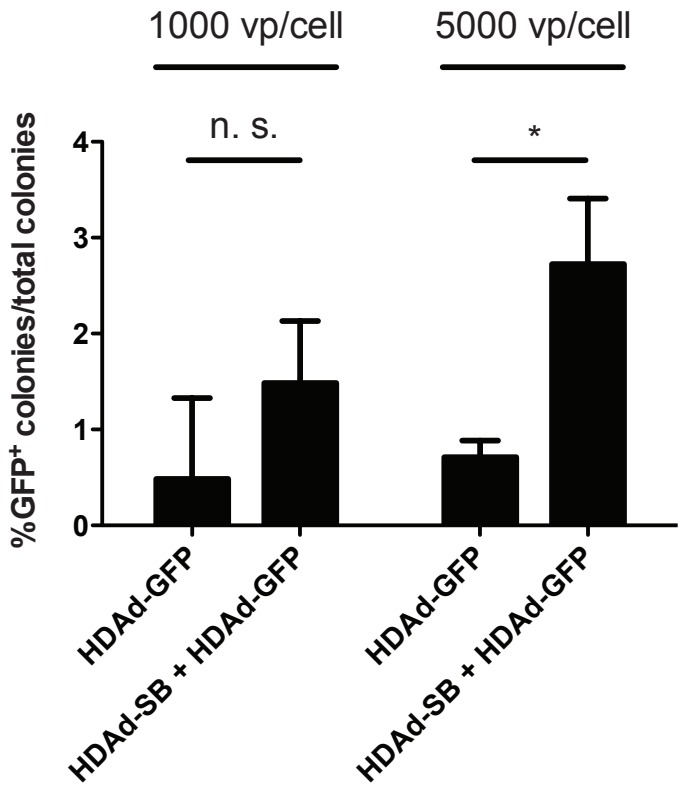

Fig. S10. Analysis of SB100x-mediated transduction of human CD34⁺ cells. CD34⁺ were infected with HDAd-GFP or HDAd-GFP + HDAd-SB at the indicated MOIs per virus and subjected to CFU assays. Shown is the mean ± SD percentage of GFP+ colonies 14 days after plating.

Supplementary Methods

Adenovirus vectors:

First-generation Ad5/35++-GFP and Ad5-GFP vectors: These Ad5-based vectors are deleted for the E1 and E3 regions and contained a 2.3-kb cytomegalovirus promoter-driven enhanced green fluorescent protein (*EGFP*) gene (derived from pEGFP-1) (Clontech, Palo Alto, CA) inserted into the E3 region. The Ad5/35++ vector contained, the short Ad35 fiber shaft and the Ad35 fiber knob with Asp207Gly and Thr245Ala amino acid substitutions instead of the Ad5 shaft and knob [1].

HDAd-GFP: Generation of the transposon vector HDAd-GFP: The plasmid pHM5-attB-T_{MCS}-FRT2 was described earlier [2]. It was modified by adding a *PacI* linker into the *Pme*I restriction enzyme site. The expression cassette encoding GFP under the control of the elongation factor alpha-1 (EF1α) promoter was released from the plasmid pEf1a-GFP by *PacI* restriction enzyme digest and ligated into the plasmid pHM5-attB-T_{MCS}-FRT2 resulting into the intermediate clone pHM5-T/EF1α-GFP-FRT2. The bacterial artificial chromosome (BAC) containing the helper-dependent Ad5 genome (B-HCA) was described earlier [3]. Based on our previously established recombineering pipeline [3], we inserted a selection marker flanked by homology arms into the BAC B-HCA and then replaced it by the transposon encoding GFP under the control of the EF1α promoter flanked by FRT sites. For recombineering, the transposon was released through the restriction enzymes *I-CeuI* and *PI-SceI* and recombined into the BAC. The new recombineering protocol is involves the selection marker *galK* which can be used for positive and negative selection. In this system, recombinases are encoded endogenously by bacteria of *E. coli* strain SW102, which express high levels upon heat-induction. In contrast to previous methods, small homologous regions (<50 bp) are sufficient for efficient recombination, which can be generated by PCR utilizing adequate primers.

HDAd-SB: The vector expressing the hyperactive SB100x has been described recently [4]. In brief, the Flp recombinase expression cassette consisting of the Ef1a promotor, the Flp recombinase cDNA and the polyA signal was PCR amplified from plasmid pFTCHSB5- Flp was used. The PCR product was cloned into the plasmid pHM5-PmeI using the restriction enzyme *Pme*I resulting in the plasmid pHM5-Flp [5]. Subsequently the cDNA of SB100X was PCR amplified from pZac-SB100 and the fragment was cloned into the *Pme*I site of pPGK-ΔTP. The SB100X expression cassette expressed under control of the PGK promoter was PCR amplified and cloned into pHM5- FLP, resulting in the plasmid pHM5-Flp-SB100. After *Cla*I digest of this plasmid, homologous arms flanking the Flp-SB100 cassette for subsequent recombinieering into pBHCA-galK-kan[3] harboring the adenoviral 52 ITR, the adenoviral packing signal Ψ, and the 3'ITR were generated by PCR using primers BHCA-Pepi-5. This PCR fragment was then inserted via galK basedcounter-selection recombineering into pBHCA-galK-kan43 replacing galK-Kan with the Flp-SB100 cassette.

HD-Ad5/35++ vector production: For the production of HDAd-SB and HDAd-GFP virus, corresponding plasmids were linearized with *PmeI* and rescued in 116 cells [6] with AdNG163-5/35++, an Ad5/35++ helper vector containing chimeric fibers composed of the Ad5 fiber tail, the Ad35 fiber shaft, and the affinity-enhanced Ad35++ fiber knob. AdNG163-5/35++ was constructed by replacing the 2,015 bp *NdeI-AflII* fragment from pAdNG163-2 [7] with the 1,259 bp *NdeI-AflII* fragment from pWE15-A2 [1]. HD-Ad5/35++ vectors were produced in 116 cells as described in detail elsewhere [6]. In brief, the liberated HD-Ad genome is transfected into 116 cells expressing Cre recombinase and and infected with the helper virus bearing a packaging signal flanked by loxP sites. Cre-mediated excision of the packaging signal renders the helper virus genome unpackagable, but still able to replicate and provide all of the necessary *trans*-acting factors for propagation of the HDAd. The titer of the HDAd is increased by serial passages on 116 cells. Finally, the HDAd is purified by CsCl ultracentrifugation. Helper virus contamination levels were found to be <0.05%. Titers were 3-9x10^{12} vp/ml.

Cells: $CD34^+$ cells were recovered from frozen stocks and incubated overnight in Iscove's modified Dulbecco's medium (IMDM) supplemented with 10% heat-inactivated FCS, 1% BSA 0.1 mmol/l 2-

mercaptoethanol, 4 mmol/l glutamine and penicillin/streptomycin, Flt3 ligand (Flt3L, 50 ng/ml), interleukin 3 (20 ng/ml), thrombopoietin, (10 ng/ml) and stem cell factor (50 ng/ml). Cytokines and growth factors were obtained from Peprot were maintained in RPMI 1640 medium containing 10% FCS, 2 mmol/l l-glutamine, Pen-Strep, and granulocyte-macrophage colony stimulating factor (GM-CSF, 0.1 ng/ml) (Peprotech, Rocky Hill, NJ).

Flow cytometry: For flow analysis of LSK cells, cells were treated with FcR blocking reagent (Miltenyi Biotec, San Diego, CA), stained with biotin-conjugated lineage detection cocktail (Miltenyi Biotec, San Diego, CA) and antibodies against c-Kit and Sca-1 as well as APC-conjugated streptavidin. Other antibodies including anti-mouse-CD3, -CD11b, -CD19, Gr-1, -CD48, -CD150 as well as anti-human-CD3, -CD19, -CD33, -CD45 and –CD46 were from BD Biosciences (Franklin Lakes, NJ) or eBioscience (San Diego, CA).

Colony-forming unit (CFU) assay: CFU assays were performed using ColonyGEL (Reachbio, Seattle, WA) human or mouse complete medium to the manufacturer's specifications. For CFU assays of *in vivo* transduced hCD46tg animals, bone marrow cells were isolated aseptically and lineage-depleted using the mouse lineage depletion kit (Miltenyi Biotec, San Diego, CA). Cells were then sorted for GFP^+ using FACS and subjected to CFU assays. Colonies were scored 12 days after plating.

Integration analysis in MO7e cells: MO7e cells were infected either with HDAd-GFP alone or with a 1:1 mixture of HDAd-SB and HDAd-GFP. Cells were cultured for 48 h to allow for transgene expression. GFP^+ cells were sorted into 96-well plates using FACS at 1 cell per well. The single clones were expanded for 2 weeks and the percentage of GFP^+ cells per colony was assessed visually using a UV microscope. Clones with the highest expression levels of GFP were selected and further expanded for integration analysis by Southern Blot. For this, genomic DNA of selected clones was isolated and digested with *SacI.* If integration of the viral genome occurred at random the digest would result in a GFP-containing fragment of 2500 bp. If the integration of the GFP cassette was mediated by the *Sleeping Beauty* transposase, GFP fragments of varying sizes would be obtained. Digested gDNA was analyzed by Southern blotting as described before [8] and detected with a CTP-labeled GFP probe. The 720 bp probe was obtained by digesting a plasmid containing the viral GFP cassette with *NcoI* and *NotI.* No specific feature within images shown in supplemental figure S2 was enhanced, obscured, moved, removed, or introduced.

qPCR for Ad genomes: Tissues were collected, and homogenized using a TissueRuptor (Qiagen, Valencia, CA). From the tissue samples, genomic DNA (gDNA) was isolated using the Blood and Tissue Kit (Qiagen, Valencia, CA) to the manufacturer's instructions and gDNA concentration was determined spectrophotometrically. gDNA samples were analyzed for vector genomes carrying a GFP cassette with the following primers: FWD: TCGTGACCACCCTGACCTAC, REV: GGTCTTGTAGTTGCCGTCGT. qPCR was performed using the Kapa SYBR Fast qPCR Kit master mix (Kapa Biosystems, Boston, MA). Each reaction was run in triplicates. Serial dilutions of purified HDAd-GFP viral DNA were used as a standard curve.

Tissue immunofluorescence analysis: Before tissue harvest, blood was flushed from the circulation with PBS using the heart as a pump. Tissues were frozen in OCT compound. Sections (6 □m) were fixed in 4% para-formaldehyde and either remained unstained or were stained with rat anti-mouse CD45 primary Ab (BD Biosciences, Franklin Lakes, NJ). Specific binding of primary Abs was visualized with secondary anti-rat Alexa Fluor 488 Ab. After washing, the slides were mounted with Vectashield containing DAPI (Vector Laboratories, Inc. Burlingame CA). Immunofluorescence microphotographs were taken at room temperature on a Leica DMLB microscope (40x oil lens) (Leica, Wetzlar, Germany) with a Leica DFC300FX digital camera and Leica Application Suite Version 2.4.1 R1 (Leica Microsystems, Heerbrugg, Switzerland).

No specific feature within images shown in supplemental figure S6 was enhanced, obscured, moved, removed, or introduced.

Construction of integration site libraries for Illumina sequencing: Amplification of SB genomic DNA junctions was performed by linear amplification-mediated PCR as described previously [9] with some modifications. Genomic DNA was isolated from GFP^+ hCD46tg colonies using the DNeasy Blood and Tissue kit (Qiagen, Valencia, CA). These CFU colonies were obtained from lin^-/GFP^+ bone marrow cells of *in vivo* transduced hCD46tg animals as described below. The isolated genomic DNA was digested with *NlaIII* or *MluCI* restriction enzymes and ligated to adaptors having *NlaIII* (annealed NlaIII+ and NlaIII- linkers) or *MluCI* (annealed MluCI+ and MluCI- linkers) compatible overhangs. Then 2 X 50 rounds of linear amplification was carried out with a biotinylated SB left inverted repeat specific primer (LAM SB-50-Bio) to enrich fragments with SB genomic junction. The single-stranded biotinylated products were captured on streptavidin-coated magnetic beads using Dynabeads kilobase BINDER kit (Invitrogen, Carlsbad, CA). After washing the beads with water, the captured products were eluted in water by incubating at 80 °C for 3 min, and used as template of nested PCRs. During amplification, we used bar-coded primers specific for the SB left inverted repeat and adapter specific primers so that we could pool different libraries in the subsequent steps (primers in PCR1: linker primer and SB-20-hmr-bio; primers inPCR2: nested primer and SB_PE_new_bc1 or bc2 or bc3). Finally, primers corresponding to Illumina adapter sequences were used (PE_nest_ind1 and Illumina1) to yield a directional library, in which sequences complementary to the Illumina genomic DNA sequences primer were located upstream to the SB left inverted repeat. The resulting libraries were pooled and sequenced on a single flow cell lane on Illumina HiSeq Genome Analyzer platform with rapid 1X100 bp single end run settings.

Linker forming	**Oligo name**	**sequence**
MluCI+	PE_Linker(+)	gtaatacgactcactatagggctccgcttaagggacgtgactggagttcagacgtgtgctcttccgatct
NlaIII+	PE_NlaIII_Linker(+)	gtaatacgactcactatagggctccgcttaagggacgtgactggagttcagacgtgtgctcttccgatctcatg
NlaIII-	PE_Linker(-)blunt	agatcggaagagcacacgtctgaactccagtcac-amino
MluCI-	PE_Linker(-)MluCI	aattagatcggaagagcacacgtctgaactccagtcac-amino
	LAM SB-50-Bio	bio-agttttaatgactccaacttaagtg
	Linker Primer	Gtaatacgactcactatagggc
	SB-20hmr-Bio	bio-aacttaagtgtatgtaaacttccgact

	Nested Primer	Agggctccgcttaagggac
	SB_PE_new_bc1	acactctttccctacacgacgctcttccgatctatcacggtatgtaaacttccgacttcaa
	SB_PE_new_bc2	acactctttccctacacgacgctcttccgatctacatcggtatgtaaacttccgacttcaa
	SB_PE_new_bc3	acactctttccctacacgacgctcttccgatctgcctaagtatgtaaacttccgacttcaa
	PE_nest_ind1	caagcagaagacggcatacgagatcgtgatgtgactggagttcagacgtgtgctcttccgatct
	Illumina 1	aatgatacggcgaccaccgagatctacactctttccctacacgacgctcttccgatct

Bioinformatic Analysis of Integration Sites: Sample-specific barcoded sequencing reads were de-multiplexed from multiplexed flow cells using CASAVA, an Illumina software suit. The quality of sequencing runs of resulting fastq files was evaluated using FastQC (http://www.bioinformatics.babraham.ac.uk/projects/fastqc). Reads were starting with the barcode GTATGTAAACTTCCGACTTCAACTG that follows the TA dinucleotide which is characteristic of SB integration were aligned against the latest version of mouse reference genome (GRCm38/mm10 (Dec, 2011)), using bowtie [10]. *Distribution of integrations:* Annotations of UTRs, Exons and CDS were downloaded from https://genome.ucsc.edu/cgi-bin/hgTables. We further extended the coordinated in silico to annotate them as shown in Fig.3f. We analyzed the percentage of integration sites overlapping with the given genomic coordinates. *Analysis for Randomness:* We performed the Bartels rank test of randomness upon the position of integration sites. This test displayed a p-value of < 2.2e-15. When we performed the same test on the distance between any two given integrations, it displayed a p-value = 0.02636 suggesting 72 percent of randomness. To create Fig.3h, we indexed and created 400 normal, shuffled and randomized windows of mouse genome mm10 using BEDtools [11]. We then counted the number of integrations for each window and plotted the density. *Integration into or near cancer-related genes:* Genes from pathways in cancer - Mus musculus (mouse) were downloaded from KEGG database (http://www.genome.jp/kegg-bin/show_pathway?mmu05200). We mapped their genomic coordinates and calculated the distance of integration sites from the closest cancer-related genes.

Animal studies: All experiments involving animals were conducted in accordance with the institutional guidelines set forth by the University of Washington.

anti-GFP antibody ELISA: Plates were coated with recombinant GFP (Clontech) (0.3μg per well in 0.1M Na-bicarbonate buffer pH9.6, o/n at 4°C). After blocking in Starting Block PBS buffer (Thermo Scientific), plates were incubated with mouse serum dilution (1:1000 in blocking buffer) followed by anti-mouse Ig-HRP conjugate. OD450 was measured and used to express antibody titers.

anti-GFP T-cell assay: CD8 T-cell responses in splenocytes harvested from mice 20 weeks after *in vivo* HSC transduction. For in vitro stimulation, splenocytes from naïve hCD46 transgenic mice (C57Bl/6 background) were transduced with HDAd-GFP (AdGFP) or an HD-Ad control (AdCo) virus (without GFP) at an MOI of 1000 vp/cell, or mock-transdcued, and cultured for three days. For the T-cell assay, cells were irradiated at 2500 Rad. Splenocytes from *in vivo* transduced mice (N=4) and one naïve mouse were harvested 20 weeks after transduction. CD8 cells were isolated using the Miltenyi MACS isolation kit. These cells were mixed with stimulator cells at a ratio of 5:1 and incubated for 5 days in the presence of 10U/ml IL-2. To measure GFP-specific T-cell activation (IFNγ production), C57Bl/6 derived TC1 cancer cells were transduced with HDAd-GFP or HDAd-Co and incubated for 3 days (designated "TC1-AdCo" and "TC1-AdGFP" target cells in the figure). Target cells were incubated with *in vitro* stimulated CD8 cells at a ratio of 1:1 and IFNγ levels in the supernatants were measured by ELISA (eBioscience) 24 hours later.

Blood analyses: Blood cell counts and blood chemistry analyses were performed by the University of Washington Medical Center laboratories. Serum levels of inflammatory cytokines were analyzed a Mouse Inflammatory Cytometric Bead Array (BD Biosciences, Franklin Lakes, NJ).

Statistical analyses: For the statistical comparison of two groups unpaired, two-sided T-tests were used. If the group variances were significantly different, Welch's correction was employed. For comparisons of multiple groups, one-way and two-way analysis of variance (ANOVA) with Bonferroni post-testing for multiple comparisons was employed. Statistical analysis was performed using GraphPad Prism version 6.01 (GraphPad Software Inc., La Jolla, CA). * $P < .05$; ** $P < .01$; *** $P < .001$, **** $P < .0001$

References:

1. Wang H, Liu Y, Li Z, et al. In vitro and in vivo properties of adenovirus vectors with increased affinity to CD46. *J Virol*. 2008;82(21):10567-10579. Prepublished on 2008/08/30 as DOI JVI.01308-08 [pii]
10.1128/JVI.01308-08.
2. Hausl MA, Zhang W, Muther N, et al. Hyperactive sleeping beauty transposase enables persistent phenotypic correction in mice and a canine model for hemophilia B. *Mol Ther*. 2010;18(11):1896-1906. Prepublished on 2010/08/19 as DOI mt2010169 [pii]
10.1038/mt.2010.169.
3. Muck-Hausl M, Solanki M, Zhang W, Ruzsics Z, Ehrhardt A. Ad 2.0: a novel recombineering platform for high-throughput generation of tailored adenoviruses. *Nucleic Acids Res*. 2015;43(8):e50. Prepublished on 2015/01/23 as DOI gkv031 [pii]
10.1093/nar/gkv031.
4. Boehme P, Zhang W, Solanki M, Ehrke-Schulz E, Ehrhardt A. A high-capacity adenoviral hybrid vector system utilizing the hyperactive Sleeping Beauty transposase SB100x for enhanced integration. *Molecular Therapy - Nucleic Acids*. 2016;5(e1):doi10.1038.
5. Yant SR, Ehrhardt A, Mikkelsen JG, Meuse L, Pham T, Kay MA. Transposition from a gutless adeno-transposon vector stabilizes transgene expression in vivo. *Nat Biotechnol*. 2002;20(10):999-1005. Prepublished on 2002/09/24 as DOI 10.1038/nbt738
nbt738 [pii].
6. Palmer D, Ng P. Improved system for helper-dependent adenoviral vector production. *Mol Ther*. 2003;8(5):846-852. Prepublished on 2003/11/06 as DOI S1525001603002855 [pii].
7. Palmer DJ, Ng P. Physical and infectious titers of helper-dependent adenoviral vectors: a method of direct comparison to the adenovirus reference material. *Mol Ther*. 2004;10(4):792-798. Prepublished on 2004/09/29 as DOI 10.1016/j.ymthe.2004.06.1013
S1525-0016(04)01308-5 [pii].

8. Wang H, Shayakhmetov DM, Leege T, et al. A capsid-modified helper-dependent adenovirus vector containing the beta-globin locus control region displays a nonrandom integration pattern and allows stable, erythroid-specific gene expression. *J Virol*. 2005;79(17):10999-11013.
9. Moldt B, Miskey C, Staunstrup NH, et al. Comparative genomic integration profiling of Sleeping Beauty transposons mobilized with high efficacy from integrase-defective lentiviral vectors in primary human cells. *Mol Ther*. 2011;19(8):1499-1510. Prepublished on 2011/04/07 as DOI mt201147 [pii]
10.1038/mt.2011.47.
10. Langmead B, Trapnell C, Pop M, Salzberg SL. Ultrafast and memory-efficient alignment of short DNA sequences to the human genome. *Genome Biol*. 2009;10(3):R25. Prepublished on 2009/03/06 as DOI gb-2009-10-3-r25 [pii]
10.1186/gb-2009-10-3-r25.
11. Quinlan AR, Hall IM. BEDTools: a flexible suite of utilities for comparing genomic features. *Bioinformatics*. 2010;26(6):841-842. Prepublished on 2010/01/30 as DOI btq033 [pii]
10.1093/bioinformatics/btq033.